NeuroImage 142 (2016) 628–644

Contents lists available at ScienceDirect

NeuroImage

journal homepage: www.elsevier.com/locate/ynimg

Left posterior-dorsal area 44 couples with parietal areas to promote speech fluency, while right area 44 activity promotes the stopping of motor responses

Nicole E. Neef [a,b,*,1], Christoph Bütfering [a,1], Alfred Anwander [b], Angela D. Friederici [b], Walter Paulus [a], Martin Sommer [a]

[a] Department of Clinical Neurophysiology, Georg-August-University, Robert-Koch-Straße 40, 37075 Göttingen, Germany
[b] Department of Neuropsychology, Max Planck Institute for Human Cognitive and Brain Sciences, Stephanstraße 1a, 03104 Leipzig, Germany

ARTICLE INFO

Article history:
Received 5 June 2016
Accepted 15 August 2016
Available online 16 August 2016

Keywords:
Broca's region
Area 44
Stuttering
Motor imagery
Automaticity
Speech motor control
Motor inhibition

ABSTRACT

Area 44 is a cytoarchitectonically distinct portion of Broca's region. Parallel and overlapping large-scale networks couple with this region thereby orchestrating heterogeneous language, cognitive, and motor functions. In the context of stuttering, area 44 frequently comes into focus because structural and physiological irregularities affect developmental trajectories, stuttering severity, persistency, and etiology. A remarkable phenomenon accompanying stuttering is the preserved ability to sing. Speaking and singing are connatural behaviours recruiting largely overlapping brain networks including left and right area 44. Analysing which potential subregions of area 44 are malfunctioning in adults who stutter, and what effectively suppresses stuttering during singing, may provide a better understanding of the coordination and reorganization of large-scale brain networks dedicated to speaking and singing in general. We used fMRI to investigate functionally distinct subregions of area 44 during imagery of speaking and imaginary of humming a melody in 15 dextral males who stutter and 17 matched control participants. Our results are fourfold. First, stuttering was specifically linked to a reduced activation of left posterior-dorsal area 44, a subregion that is involved in speech production, including phonological word processing, pitch processing, working memory processes, sequencing, motor planning, pseudoword learning, and action inhibition. Second, functional coupling between left posterior area 44 and left inferior parietal lobule was deficient in stuttering. Third, despite the preserved ability to sing, males who stutter showed bilaterally a reduced activation of area 44 when imagine humming a melody, suggesting that this fluency-enhancing condition seems to bypass posterior-dorsal area 44 to achieve fluency. Fourth, time courses of the posterior subregions in area 44 showed delayed peak activations in the right hemisphere in both groups, possibly signaling the offset response. Because these offset response-related activations in the right hemisphere were comparably large in males who stutter, our data suggest a hyperactive mechanism to stop speech motor responses and thus possibly reflect a pathomechanism, which, until now, has been neglected. Overall, the current results confirmed a recently described co-activation based parcellation supporting the idea of functionally distinct subregions of left area 44.

1. Introduction

In 1861, Broca assigned a region in the human left frontal lobe to a designated function – articulated language. More than 150 years later, it is still an open question, how the human brain generates well-organized, fluent speech. The most famous functions of Broca's area consider operations of speech production, ranging from semantic, to syntactic, and phonologic processing (Amunts et al., 2004; Eickhoff et al., 2009; Flinker et al., 2015; Friederici, 2011; Heim et al., 2008; Heim et al., 2010; Price, 2010; Sahin et al., 2009). Besides, this region is engaged in domain-general functions including hierarchical structure building (Sakai and Passingham, 2006), aspects of action processing (Nishitani and Hari, 2000), rhythm and music processing (Platel et al., 1997), working memory processing (Buchsbaum et al., 2005; Fiebach et al., 2005; Ranganath et al., 2003), or cognitive control (Koechlin and Summerfield, 2007). Recent theories postulate a rostral-to-caudal gradient for structured sequence processing (Uddén and Bahlmann, 2012) and degree of automaticity (Jeon and Friederici, 2015) stretching from orbital area 47, to area 45 and 44 over the whole left inferior

* Corresponding author at: Department of Neuropsychology, Max Planck Institute for Human Cognitive and Brain Sciences, Stephanstraße 1a, 04103 Leipzig, Germany.
E-mail addresses: nneef@gwdg.de (N.E. Neef), christoph.buetfering@gmail.com (C. Bütfering), anwander@cbs.mpg.de (A. Anwander), friederici@cbs.mpg.de (A.D. Friederici), wpaulus@med.uni-goettingen.de (W. Paulus), msommer@gwdg.de (M. Sommer).
[1] These authors contributed equally.

http://dx.doi.org/10.1016/j.neuroimage.2016.08.030

frontal gyrus (IFG). Across cognitive domains including language, music and action, it has been suggested that more abstract control demanding components of action are supported by anterior prefrontal regions, whereas, with increasing degree of automaticity, concreteness, and, thus, temporally proximity more posterior regions are likely to be involved (Badre, 2008; Jeon and Friederici, 2013).

Growing evidence consolidates morphological and physiological subdivisions of Broca's area. Cytoarchitectonically, anatomists distinguish anterior area 45 and posterior area 44 (Aboitiz and García, 1997; Amunts et al., 1999; Brodmann, 1909). Macroanatomic landmarks give a coarse estimation of where these areas are settled. However, real locations vary between subjects. The anatomical organization of Broca's region has been detailed in the seminal works by Amunts and colleagues (Amunts et al., 1999, 2010). Area 45 occupies the pars triangularis of the IFG with a rostral border to area 47 occupying the orbital part of the IFG. Dorsally area 45 and area 44 border on areas in the inferior frontal sulcus, ventrally opercular areas adjoin area 45 and area 44 at varying positions at the entrance of the Sylvian fissure. The border between area 45 and area 44 has been described within the ascending branch of the lateral fissure or between the diagonal sulcus and ascending branch on the cortical surface of the IFG. Area 44 is settled in the pars opercularis of the posterior IFG, anterior to area 6 on the precentral gyrus. These areas differ with respect to size and laminar distribution of neurons (cytoarchitectonics) suggesting different attributions to brain function. Results from diffusion-weighted magnetic resonance imaging are complementary to this. Based on probabilistic tractography, Broca's area was segregated into three cortical areas with mutually distinct and internally coherent connectivity reminiscent of the cytoarchitctonic parcellation (Anwander et al., 2007). Receptorarchitectonically, area 45 can be further subdivided into an anterior (area 45a) and posterior (area 45p) part; area 44 can be further subdivided into a dorsal (area 44d) and a ventral (area 44v) part (Amunts et al., 2010), because neurotransmitter receptors are expressed at largely varying density across these parts.

An additional operative segmentation was suggested by a recent functional connectivity analysis reporting five functionally different subdivisions of left area 44 (Fig. 1) (Clos et al., 2013). Theses subdivisions build the regions of interest (ROI) of the current work. Clos and colleagues obtained this segmentation by a connectivity-based parcellation as a way of meta-analytic connectivity modelling (Laird et al., 2009). Thereby, area 44 was used as a seed region in a brain template (Amunts et al., 1999, 2004; Evans et al., 2012). Co-activation patterns of area 44 were subsequently extracted from a large data base, the BrainMap database (https://www.brainmap.org/), considering several thousand imaging experiments from pure mapping studies in healthy subjects. To delineate the brain networks that are co-active across many different experimental tasks, an algorithm computed the convergence across all reported foci of all BrainMap experiments, where the seed region in question was reported to be active. Eventually, the seed region was clustered into different subdivisions based on similarities and differences in the co-activation profile (Cieslik et al., 2013; Laird et al., 2009). Due to the co-activation based parcellation analysis the region specific information processing of area 44 can be roughly described as following. Three anterior clusters (Fig. 1, C2, C3, and C5) were primarily associated with language and cognition, and two posterior clusters (Fig. 1, C1 and C4) were primarily associated with action processes such as imagined movements, articulation of speech, and rhythmic sequencing (Clos et al., 2013). In the following, area 44pd refers to the posterior-dorsal cluster 1 and area 44pv refers to posterior-ventral area 44.

Stuttering is associated with various neuronal changes throughout cortical and subcortical networks. For a recent review see (Neef et al., 2015a). The left prefrontal cortex is a brain region often associated with stuttering as well as its remediation (Belyk et al., 2015; Kell et al., 2009; Neumann et al., 2005) and has been considered as the region with an etiologic role for stuttering (Lu et al., 2012). In particular, left area 44 is a neural correlate of stuttering. Grey matter probability matures irregularly (Beal et al., 2015; Beal et al., 2013; Chang et al., 2008), which is still evident in adulthood (Kell et al., 2009; Lu et al., 2012). Various speech tasks elicit aberrant activation patterns (Braun et al., 1997; Ingham et al., 2012; Lu et al., 2012; Salmelin et al., 2000; Toyomura et al., 2011; Wymbs et al., 2013), resting state functional connectivity is diminished (Lu et al., 2012), and functional connectivity between left area 44 and the adjacent premotor cortex is reduced during speech tasks (Chang et al., 2011). Here we investigated whether the trait of stuttering can be associated with a particular subdivision of area 44. To achieve this aim, we conducted a functional magnetic

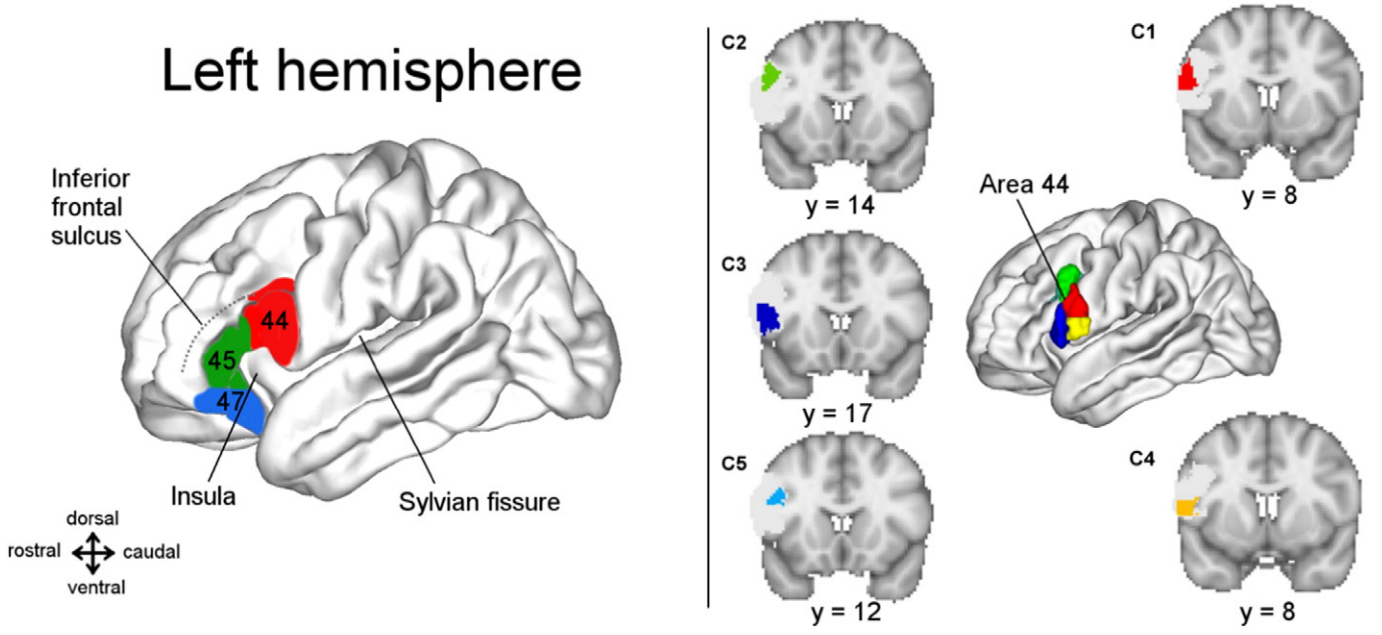

Fig. 1. Area 44 parcels. The surface mesh of the left hemisphere of the MNI standard brain on the left shows the inferior frontal gyrus and the approximate location of Brodmann areas 44, 45, and 47. Coronal slices on the right display the Juelich probability map of area 44 (Amunts et al., 1999, 2004) in light-grey. Functionally distinctive area 44 clusters that resulted from a co-activation based parcellation (Clos et al., 2013) are displayed separately on these coronal slices posterior (y = 8) to anterior (y = 17). The surface mesh of the left hemisphere of the MNI standard brain shows the collocation of all clusters in left area 44 in the middle.

resonance imaging study (fMRI) and extracted blood oxygenation level dependent responses (BOLD) from the five subregions of area 44.

Fluent speech production requires planning, selection, and sequencing of motor control signals, orchestrating a complex muscle system, thereby generating the continuous flow of speech. While speaking, stuttering occurs in the form of involuntary sound and syllable repetitions, prolongations or blocks. Some theories on stuttering propose that earlier speech planning mechanisms are affected (Howell and Au-Yeung, 2002; Max et al., 2004; Walsh et al., 2015). Neuroimaging methods with a high time resolution provide evidence for this hypothesis. An MEG study showed a reversed timing pattern of the cascade of neuronal activity that usually propagates from preparatory left precentral regions towards the executing primary motor sites; in stuttering, however, primary motor sites were more active at a very early stage of speech motor preparation (Salmelin et al., 2000). A recent study from our lab showed that a speech-planning related left-lateralized excitability increase of the speech motor cortex was absent in adults who stutter (AWS) (Neef et al. 2015b), which might be caused by a deficient functional coupling between the left primary motor cortex, the left premotor cortex, and left area 44 (Chang et al., 2011). This notion is supported by theories and models postulating left area 44 to be one of the core cortical hubs in the network of speech-planning-related operations (Bohland et al., 2009; Flinker et al., 2015; Guenther and Hickok, 2015).

A remarkable phenomenon accompanying stuttering is the preserved ability to sing (Andrews et al., 1982). Speaking and singing are connatural behaviours recruiting largely overlapping brain networks (Callan et al., 2006; Koelsch et al., 2002; Özdemir et al., 2006). Analysing what effectively suppresses stuttering while singing may provide a better understanding of the pathophysiology of stuttering itself. An early imaging study relates singing and other fluency-enhancing techniques to robust increases of activity in left hemisphere fronto-parieto-temporal substrates along with the putamen (Stager et al., 2003), suggesting a facilitating effect of a more effective coupling between auditory and motor functions. Here, we chose two motor imagery tasks, imagine speaking an over-learned vocal sequence, specifically the months of the year, and imagine humming a non-verbal tune, specifically Mozart's "Eine kleine Nachtmusik" (Serenade No. 13 for strings in G major), adopted by (Riecker et al., 2000). The induced motor simulation processes neglect an auditory-to-motor coupling but likely reflect motor preparation without execution (Bohland and Guenther, 2006; Palmer et al., 2001; Tian et al., 2016) and thus should significantly involve area 44 (Gunji et al., 2007). Given the preserved ability to sing, it was plausible to hypothesize comparable activation patterns in fluent speakers and AWS in the melody humming task. Contrastingly, the speaking task was expected to elucidate area's 44 signatures of stuttering. It is crucial to note that participants were not instructed to imagine stuttering but to imagine speaking fluently a highly automatized word list. This is an easy task and clinical observations show that AWS often manage this fluently when actually speaking (Bloodstein and Ratner, 2008). Importantly, the assumption here was not that AWS naturally imagine stuttering. Hence, the recruited network likely reflects processes of speech motor planning e.g. (Tian et al., 2016). The underlying presumption is that actual stuttering is only the tip of the iceberg of an anyway vulnerable speech motor system (Kent, 2000; Ludlow, 2000; Smith and Kelly, 1997; van Lieshout et al., 2004). Thus, the crucial aspect of the current study question is that not actual speaking but such a preparatory process is related to a possibly altered function of left area 44. An additional aspect of this approach was the avoidance of motion artifacts as well as physiological artifacts in the fMRI signal that are likely to occur during vocal production (Callan et al., 2006). We analyzed data from dextral, aged-matched males to avoid interference of effects of handedness (Geschwind et al., 2002) or sex (Ingham et al., 2004; Murphy et al., 1996). The present study disentangled parcels of left area 44 that fundamentally contribute to the trait of stuttering especially during speech motor simulation and vocal motor simulation. The processes studied did not involve actual speaking and humming or speaking- and vocalization-related auditory-motor integration.

2. Material and methods

2.1. Participants

Data were analyzed from 32 native German-speaking males, 15 AWS (19–63 years, mean age 37.3 years, SD = 13.1) and 17 fluent speakers (20–62 years, mean age 37.6 years, SD = 14.0). These data were derived from a study that included a larger population addressing the question of the effect of sex on brain structure and function in AWS (Bütfering, 2015; Neef, 2013). A publication of these data is currently under preparation. To adequately address the study question, we included only the analysis of the images of male participants. Apart from stuttering in the group of AWS, participants reported no medical history, neurological impairment, or drug use that would potentially affect their neurological function. AWS were recruited from stuttering support groups. Fluent speakers were recruited via advertisements. Groups were matched for age, handedness (Oldfield, 1971), and years of formal education (1 = school; 2 = high school; 3 = <2 years college; 4 = 2 years college; 5 = 4 years college; 6 = postgraduate). Nine AWS reported a family history of stuttering. None of the fluent speakers reported a family history of speech or language disorders. All subjects provided written informed consent prior to inclusion in the study. Ethical approval from the local ethical committee at the University Medical Center Goettingen and written-informed consent were obtained prior to the investigation. Subjects were each paid 20 Euros for participating.

Stuttering severity was assessed by collecting samples of speech read aloud and from spontaneous speech elicited through a standardized interview, where participants were asked to narrate their daily routine, describe their favourite movie or novel, and give directions when asked the way. These samples were video recorded and analyzed offline by a qualified speech and language pathologist who was unaware of the diagnosis. The stuttering severity index (SSI-4) was employed to determine the frequency and duration of stuttered syllables as well as physical concomitants of stuttering (Riley, 2008). According to SSI-4, six participants showed very mild stuttering, three were mild, one was severe, and two were very severe. Three participants had an SSI score lower than 10, but were included in the analysis because they stuttered consistently during more stressful situations, such as a follow-up phone call. Table 1 summarizes the demographic information of the participants, and Table 2 reports individual characteristics of all participants.

2.2. Experimental procedure

Fig. 2 illustrates the stimulus material and time flow of the two tasks implemented in a slow-event-related design. Stimuli were presented via LCD goggles (VisuaStim XGA, Resonance Technology Inc., Northridge, CA, USA). Speech motor imagery required naming the months of the year. Melody motor imagery required the reproduction

Table 1
Participants demographic information and behavioural results.

	Stuttering	Controls	Difference
N	15	17	n/a
Age (years)	36.7 (13.3)	37.6 (14.0)	$p = 0.9$ (n.s.)
Age of stuttering onset (years)	4.5 (1.6)	n/a	n/a
SSI-4 overall score	15.6 (10.8)	n/a	n/a
% stuttered syllables	10.7 (20.4)	0.1 (0.1)	$p < 0.001$
Handedness (LQ)	89.7 (13.3)	95.6 (8.5)	$p = 0.19$ (n.s.)
Formal education	5	5	$p = 0.96$ (n.s.)

All values are group averages with the standard deviation in brackets, but education is reported as median, SSI-4 = Stuttering Severity Instrument (Riley, 2008); % stuttered disfluencies = stuttered syllables occurring per 100 syllables in a sample of 1000 syllables; LQ = laterality quotient, n.s. = not significant. All group differences were tested by Mann-Whitney *U* tests, but education was tested by an independent samples median test.

Table 2
Participants individual characteristics.

ID	Sex	Age	LQ	Edu	History	%SS	SSI	Severity	ASO
C1	m	24	100	4	None				
C2	m	26	100	5	None				
C3	m	52	100	6	None				
C4	m	36	100	6	None				
C5	m	25	80	5	None				
C6	m	26	80	5	None				
C7	m	36	100	6	None				
C8	m	27	100	6	None				
C9	m	23	100	4	None				
C10	m	47	75	1	None				
C11	m	39	100	5	None				
C12	m	56	100	6	None				
C13	m	53	95	2	None				
C14	m	30	100	6	None				
C15	m	20	95	3	None				
C16	m	57	100	1	None				
C17	m	62	100	6	None				
S1	m	27	80	5	Mother	1.3	8	Disclosed*	6
S2	m	23	80	3	None	69.6	40	Very severe	4
S3	m	50	100	6	Uncle	3.9	14	Very mild	4
S4	m	63	70	6	Uncle	2.4	12	Very mild	6
S5	m	36	60	1	Father/cousin	3	19	Mild	5
S6	m	42	100	6	Brother	1	10	Very mild	4
S7	m	27	100	5	Brother	2.3	19	Mild	9
S8	m	52	95	6	n/a	0.9	4	Disclosed*	3
S9	m	26	100	4	Grandmother	2.4	13	Very mild	4
S10	m	55	100	1	None	1.5	12	Very mild	4
S11	m	19	75	1	None	2.3	11	Very mild	5
S12	m	30	90	6	None	49.1	43	Very severe	3
S13	m	38	95	6	Father	7.9	22	Mild	3
S14	m	38	100	6	None	0.2	0	Disclosed*	4
S15	m	24	100	4	Father/brother	11.95	34	Severe	4

LQ = laterality quotient (Oldfield, 1971), Edu = education, History = family history of stuttering, %SS = stuttered syllables occurring per 100 syllables across 1000 syllables (reading and free production), SSI = stuttering severity index (SSI-4) overall score, ASO = age of stuttering onset in years, *disclosed = SSI-4 does not give a diagnosis of stuttering but participants reported their history of stuttering and disclosed continuing stuttering.

of the non-lyrical tune drawn from a serenade (W.A. Mozart's, Eine kleine Nachtmusik, KV 525). A trial was initiated by presenting a visual cue, the letter "J", as a prompt for participants to imagine speaking or a note prompting them to imagine humming a melody. After 6 s, a plus symbol signalled participants to stop imagining and rest for the following 18 s. Twenty-four trials were randomly presented in a run with 12 repetitions per condition. A run lasted 10 min. Every participant, except two AWS, performed three blocks resulting in 36 trials per condition. The two AWS finished only 2 blocks. For them, task-related BOLD responses were averaged across the two available runs. The task was adopted from (Riecker et al., 2000). Prior to the experiment, participants listened to the melody and performed the tasks outside the scanner to familiarize them with the test materials.

2.3. Magnetic resonance imaging

Magnetic resonance imaging was conducted in a 3-T (Tim Trio, Siemens Healthcare, Erlangen, Germany) using an 8-channel head coil for signal reception. Subjects were positioned supine inside the magnet bore. Initially, structural whole-brain T1-weighted MRI involved a non-selective inversion-recovery 3D turbo FLASH sequence (TR = 2250 ms, TE = 3.26 ms, flip angle = 9°, TI = 900 ms) at 1 mm^3 isotropic spatial resolution. All fMRI measures were based on a gradient-echo EPI sequence (TR = 2000 ms, TE = 30 ms, flip angle 70°) at a 3 mm^3 isotropic spatial resolution. We acquired 33 consecutive slices positioned roughly parallel to the intercommissural plane, thereby covering the whole brain [64 × 64 × 33]. All images were corrected for motion in k-space as supplied by the manufacturer (Siemens Healthcare, Erlangen, Germany). These motion corrected images were used for off-line whole-volume analysis.

2.4. Data analyses

2.4.1. Pre-processing and whole-brain fMRI analysis

FMRI data processing was carried out using FEAT version 6.0, a tool from the FMRIB Software library (FSL; http://fsl.fmrib.ox.ac.uk). Preprocessing involved an additional motion correction by image-based registration (Jenkinson et al., 2002), smoothing with a Gaussian kernel of 8 mm full width at half maximum. Non-brain tissue was removed (Smith, 2002) and all volumes were intensity-normalized by the same factor. Temporal high-pass filtering was achieved by Gaussian-weighted least-squares straight line fitting, with a high-pass filter cut-off at 100 s. Functional images were spatially normalized to their respective anatomical image by an affine registration (Jenkinson and Smith, 2001). A further non-linear registration served to align functional images and the standard MNI152 template brain (Andersson et al., 2010). Boxcar models were convolved with a Gamma function. Model fit was determined by statistical time-series analysis in the framework of the general linear model. A fraction of the temporal derivative of the blurred original waveform was added to achieve a slightly better fit to the data. Across the three runs, within-subject contrasts of imagine speaking and rest, and imagine melody humming and rest were calculated with a fixed-effects analysis. Across participants, mixed-effects group analyses were calculated. Z (Gaussianised T/F) statistic images were thresholded using clusters determined by $Z > 3.1$ and a corrected cluster significance threshold of $p = 0.05$ (Worsley et al., 1996).

2.4.2. Regions of interest analyses in area 44

Region of interest analyses in left area 44 was based on the 5 cluster resolution of a co-activation-based parcellation as shown in Fig. 1 (Clos et al., 2013). The corresponding NIfTI files are available under the following link: http://www.fz-juelich.de/SharedDocs/Downloads/INM/INM-1/DE/Area44_Parcellation.html?nn=1277240. Clusters are normalized to MNI space and numbered correspondingly to the parcellation described in the paper by Clos and colleagues (Fig. 1). Here, time courses of the filtered functional data were extracted separately for every cluster. Subsequently, time courses were epoched between −2 and 24 s of a trial and averaged across conditions, speaking or humming, by a custom written matlab script (The MathWorks,Natick, MA). Finally, we calculated the ratio between signal intensity at the first volume (−2 to 0 s) and the following volumes. Thus, percent signal change indicated the change of signal intensity related to that of the first volume in every trial.

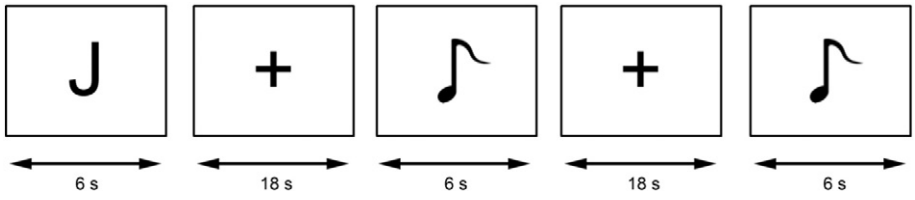

Fig. 2. Illustration of the stimuli prompting the participants to imagine speaking (letter J), to imagine humming a melody (note), or to stop imagine and rest (plus).

2.4.3. Connectivity analysis seeding in left posterior area 44

To test whether coupling between left area 44 subregions and task related brain regions was different between groups we employed connectivity analyses similar to a psychophysiological interaction (PPI) (Friston et al., 1997). The PPI analysis was carried out using FEAT version 6.0 (FSL; http://fsl.fmrib.ox.ac.uk). The two posterior clusters of left area 44 served as seed regions. We took these two clusters because they showed the highest activation level in the previous analyses. Extracted time courses were fed into the model as a regression variable (physiological component) in addition to the regression variables defining the task conditions (psychological component). PPIs were calculated as an interaction between the respective task condition and seed activity. For every run, four PPIs were calculated separately for seed region (left area 44pd, area 44pv) and task (imagery of speaking, imagery of humming a melody). Subsequent higher-level fixed effects analysis served to calculate PPI contrast maps for a conjunction of both tasks. The resulting parameter estimate images were then compared between groups at random effects level. Z (Gaussianised T/F) statistic images were thresholded using clusters determined by $Z > 2.3$ and a corrected cluster significance threshold of $p = 0.05$ (Worsley et al., 1996).

2.4.4. Regions of interest analyses in right area 44

To achieve region of interest analyses in right area 44, it was necessary to determine homologue areas. Therefore, two additional functional connectivity analyses were calculated, one for left cluster 1 and another for left cluster 4. We took these two clusters because they showed the highest activation level in the previous analyses. First- and higher-level Feat analyses were recalculated with the time courses of these clusters as an additional physiological regression variable in the model (O'Reilly et al., 2012). The mean group contrast maps of the positive correlation between the time course and all other voxels were thresholded until a cluster size was achieved that was comparable to that in the left hemisphere. Resulting cluster masks were again employed to extract the time courses and to determine the beta estimates.

Spearman rank correlation analyses were calculated to determine associations between magnitude of activation in the region of interest and stuttering severity.

Statistical analyses were performed in SPSS (IBM Corp. Released 2013. IBM SPSS Statistics for Windows, Version 22.0. Armonk, NY: IBM Corp.). For all imaging results we identified macroanatomical brain regions as well as the cytoarchitectonic areas corresponding to the MNI coordinates of activation by using the probabilistic atlases included with FSL (Desikan et al., 2006; Eickhoff et al., 2005; Lancaster et al., 2000).

3. Results

3.1. Imagery of speaking and humming involved bilateral fronto-parieto-temporal networks including basal ganglia, thalamus, and cerebellum

Participants performed two imagery tasks in the scanner, speaking and humming a melody. Contrast maps across all participants revealed similar task-related networks involving cortical and subcortical areas as reported in Table 3 (imagine speaking > rest) and in Table 4 (imagine humming > rest). Fig. 3 shows the corresponding contrast images. Speaking-related activations and humming-related activations are rendered on the brain surface as well as on two axial sections visualizing the striatum and the cerebellum, respectively. Hence, both imagery tasks activated broad fronto-parieto-temporal networks including the motor cortex, bilaterally, together with the premotor cortex, the IFG, operculum, insula, supplementary motor area, inferior parietal lobule, the supramarginal gyrus, posterior superior temporal gyrus, superior temporal sulcus, middle temporal gyrus occipital cortex, putamen and globus pallidus, thalamus, red nucleus, and cerebellum. Further activations involved the middle frontal cortex especially while imagine speaking. Additionally, the tasks broadly recruited visual areas.

Table 3
MNI coordinates of cluster maxima and local maxima while imagine speaking derived from a mixed-effects analysis across all participants.

Region	Cytoa	x	y	z	Peak Z	Voxels
L frontal pole		−30	48	28	4.69	100
R frontal pole		26	58	−6	4.42*	37
R frontal pole	9	36	50	34	5.42	292
➢ L middle frontal gyrus	8	46	34	38	4.08	
L frontal operculum	13	−34	20	6	7.20	2398
➢ L premotor cortex	6	−52	−4	48	7.07	
➢ L premotor cortex	6	−42	0	36	6.27	
➢ L anterior insula		−40	12	0	6.25	
➢ L inferior frontal gyrus	44/45	−50	12	−2	5.82	
➢ L inferior frontal gyrus pars opercularis	44	−48	8	22	5.18	
R anterior insula		32	20	8	6.98	1962
➢ R inferior frontal gyrus pars opercularis	44	42	16	6	6.58	
➢ R premotor cortex	6	56	2	46	5.90	
➢ R premotor cortex	6	52	4	50	5.86	
➢ R middle frontal gyrus	6	46	4	54	5.67	
➢ R middle frontal gyrus	6	42	4	58	5.52	
R supplementary motor area	6	6	6	64	8.26	1972
➢ L supplementary motor area	6	−4	0	66	8.22	
➢ R superior frontal gyrus		14	0	64	6.74	
➢ L paracingulate gyrus	24	−6	8	46	6.25	
➢ R paracingulate gyrus	32	4	18	42	5.42	
L anterior intraparietal sulcus	hIP3	−32	−52	46	6.40	1418
➢ L anterior intra−parietal sulcus	hIP1	−36	−46	44	5.80	
➢ L superior parietal lobule	7 A	−24	−68	48	5.35	
R superior parietal lobule	7P	30	−66	42	6.58	1735
➢ R precuneous	7 A	10	−70	42	6.13	
➢ R anterior intra−parietal sulcus	hIP1	42	−48	44	5.69	
➢ R supramarginal gyrus	PF	52	−40	−54	5.55	
➢ R anterior intra−parietal sulcus	hIP1	36	−56	44	5.08	
R posterior cingulate gyrus	23	4	−30	30	6.02	216
R inferior parietal lobule	PFm	60	−40	16	5.41	527
➢ R middle temporal gyrus		48	−26	−6	4.52	
➢ Posterior superior temporal gyrus		52	−32	2	4.28	
L parietal opercular cortex	PFm	−54	−40	22	5.90	400
➢ L middle temporal gyrus		−52	−50	10	5.03	
L superior temporal gyrus	22	−70	−26	4	4.12*	15
R middle temporal gyrus		58	−46	−8	3.89*	35
L occipital fusiform gyrus		−42	−66	−12	7.02	3113
➢ L occipital fusiform gyrus		−38	−68	−16	6.96	
➢ L lateral occipital cortex V4		−40	−90	4	6.67	
➢ L temporal occipital fusiform cortex		−34	−58	−22	6.10	
R occipital pole V1		16	−98	6	7.55	4057
➢ R lateral occipital cortex V4		38	−78	−12	7.45	
➢ R occipital fusiform gyrus		38	−70	−12	7.17	
➢ R temporal occipital fusiform cortex		36	−50	−18	7.05	
L lingual gyrus	18	−4	−88	−10	6.07	374
➢ L occipital pole	17	−8	−100	4	5.95	
L thalamus		−12	−16	8	3.39*	16
R thalamus anterior nucleus		10	−12	14	4.07*	21
R thalamus ventral lateral nucleus		12	−12	2	3.67*	11
R brainstem		8	−28	−4	4.08*	137
➢ R red nucleus		6	−16	−8	3.86*	
➢ L red nucleus		−2	−18	−6	3.54*	
L putamen		−20	4	4	4.31*	
R putamen		24	6	4	4.83*	
L cerebellum		−30	−54	−28	4.04	
R cerebellum		36	−50	−26	6.01	

Z-statistics were thresholded using clusters determined by $Z > 3.1$ and a corrected cluster significance threshold of $p = 0.05$ (Worsley, 2001). *Uncorrected *Z*-values

3.2. Imagery of speaking and humming recruited the left posterior area 44 with a reduced activation of the posterior dorsal part in stuttering

Here, we investigated, which part of left area 44 contributed most to the trait of stuttering. To achieve our aim, we extracted the task-related time courses from five functionally distinct clusters of area 44 (Clos

Table 4
MNI coordinates of cluster maxima and local maxima while imagine humming a melody derived from a mixed-effects analysis across all participants.

Region	Cytoa	x	y	z	Peak *Z*	Voxels
L frontal pole		−32	50	32	5.44	133
L anterior insula		−34	22	4	6.88	859
➢ L inferior frontal gyrus pars opercularis	44	−56	2	18	4.08	
➢ L inferior frontal gyrus pars opercularis	44	−50	8	18	4.07	
R frontal operculum		34	22	6	6.19	648
➢ R inferior frontal gyrus pars opercularis	44	48	10	0	4.66	
➢ R inferior frontal gyrus pars opercularis	44	56	14	4	4.66	
➢ R inferior frontal gyrus pars orbitalis	47	48	20	−6	4.16	
L premotor cortex	6	−52	−4	50	6.79	514
➢ L middle frontal gyrus		−42	−2	60	5.24	
➢ L premotor cortex	6	−44	−6	62	4.98	
R premotor cortex	6	52	2	44	6.33	584
➢ R middle frontal gyrus		40	6	62	4.92	
R supplementary motor area	6	2	2	68	7.28	1336
➢ L supplementary motor area	6	−4	2	68	7.11	
➢ L/R paracingulate gyrus		0	12	42	5.96	
➢ L anterior cingulate gyrus		−4	14	32	5.76	
L superior parietal lobule	7A	−34	−60	56	5.51	409
➢ L anterior intraparietal sulcus	hIP3	−30	−50	42	5.31	
➢ L superior parietal lobule	7A	−32	−56	50	5.31	
L inferior parietal lobule	PFm	−52	−40	22	5.50	149
R supramarginal gyrus		52	−38	12	5.40	667
➢ L inferior parietal lobule	PF	58	−38	20	5.40	
➢ L supramarginal gyrus		52	−42	10	5.37	
➢ L posterior superior temporal gyrus		52	−32	0	4.72	
R posterior cingulate gyrus		2	−32	28	5.78	224
R lateral occipital cortex		42	−72	−8	7.58	11,689
➢ L lateral occipital cortex		−40	−84	−4	7.49	
➢ R temporal occipital fusiform gyrus		36	−50	−20	7.33	
L putamen		−22	6	4	3.36*	
R putamen		22	6	2	4.75*	
R thalamus		12	−12	2	3.21*	

Z-statistics were thresholded using clusters determined by $Z > 3.1$ and a (corrected) cluster significance threshold of $p = 0.05$ (Worsley, 2001). *Uncorrected *Z*-values.

et al., 2013). These clusters are rendered on the brain surface of the left hemisphere (Fig. 1). In the MNI standard brain with a spatial resolution of $(2\ mm)^3$ the five clusters take up a volume of 7824 mm^3 (978 voxels; cluster 1 = 1656 mm^3, 207 voxels, centre-of-gravity [x = −56,y = 8, z = 21]; cluster 2 = 1304 mm^3, 163 voxel, centre-of-gravity [x = −51, y = 14, z = 34]; cluster 3 = 1872 mm^3, 234 voxel, centre-of-gravity [x = −52, y = 18, z = 10]; cluster 4 = 1536 mm^3, 192 voxel, centre-of-gravity [x = −56, y = 8, z = 10]; cluster 5 = 1456 mm^3, 182 voxel, centre-of-gravity [x = −45, y = 12, z = 26]). Fig. 4 displays grand-average time courses of BOLD responses separated for group, cluster, and task. The two posterior clusters (*C*1, left area 44pd and *C*4, left area 44pv) showed the largest responses in both groups and both tasks. AWS showed comparably smaller BOLD responses in the posterior-dorsal cluster 1 during both tasks.

Statistical analyses were performed on parameter estimates. To test variance between groups (Controls and AWS) and across modes (Speaking and Humming) we calculated 2 × 2 mixed-model ANCOVAs separately for each cluster. Fluency served as covariate. ANCOVA of cluster 1 yielded an effect of Group, $F(1,27) = 8.67$, $p = 0.006$, $\eta_p^2 = 0.23$, with a covariance of fluency, $F(1,27) = 5.30$, $p = 0.029$, $\eta_p^2 = 0.155$. In addition, ANCOVA revealed an effect of Mode, $F(1,27) = 18.27$, $p < 0.001$, $\eta_p^2 = 0.387$, but no interactions. ANCOVAs of cluster 2, cluster 4, and cluster 5 yielded effects of Mode (*C*2, $F(1,27) = 4.62$, $p = 0.004$, $\eta_p^2 = 0.137$; *C*4, $F(1,27) = 6.77$, $p = 0.014$, $\eta_p^2 = 0.189$; *C*5, $F(1,27) = 20.54$, $p < 0.001$, $\eta_p^2 = 0.415$), but no other effects or interactions. ANCOVA of cluster 3 yielded no effects.

Altogether, statistical analyses indicated differences in activation caused by the task. Posterior clusters 1 and 4 as well as anterior clusters 2 and 5 showed higher activations while speaking compared to humming. This task-related effect was independent of the trait of stuttering. Only cluster 1 showed a significant effect of stuttering. AWS showed a decreased activation in this area, compared to controls. This decrease was not restricted to imagine speaking. Imagine humming a melody showed a likewise decreased BOLD response.

Spearman rank correlations were calculated between stuttering characteristics and magnitude of activation in all subregions of left area 44. Cluster 2, cluster 3, and cluster 5 showed no correlations with stuttering characteristics. Speaking-related activity of left area 44pd (cluster 1) was positively correlated with percent stuttered syllables while reading ($r_{44pd} = 0.569$, $p_{44pd} = 0.027$), and showed a trending correlation with percent stuttered syllables during free speech production ($r_{44pd} = 0.501$, $p_{44pd} = 0.057$) and stuttering severity (SSI-score, $r_{44pd} = 0.483$, $p_{44pd} = 0.068$). Humming-related activity in left area 44pd showed a trending correlation with percent stuttered syllables while reading ($r_{44pd} = 0.496$, $p_{44pd} = 0.060$) and no correlation with percent stuttered syllables during free speech production ($r_{44pd} = 0.387$, $p_{44pd} = 0.154$) or stuttering severity (SSI-score, $r_{44pd} = 0.428$, $p_{44pd} = 0.112$). Speaking-related activity of left area 44pv (cluster 4) was positively correlated with percent stuttered syllables while reading ($r_{44pv} = 0.659$, $p_{44pv} = 0.008$) and stuttering severity (SSI-score, $r_{44pv} = 0.531$, $p_{44pv} = 0.042$), and no correlation occurred with percent stuttered syllables during free speech production ($r_{44pv} = 0.235$, $p_{44pv} = 0.356$). Humming-related activity of left area 44pv correlated positively with percent stuttered syllables while reading ($r_{44pv} = 0.587$, $p_{44pv} = 0.021$), and stuttering severity ($r_{44pv} = 0.555$, $p_{44pv} = 0.032$), and not with percent stuttered syllables during free speech production ($r_{44pv} = 0.211$, $p_{44pv} = 0.343$).

3.3. Left posterior-dorsal area 44 coupled with parietal areas in fluent speakers, but not in AWS

The two posterior clusters of left area 44 showed the strongest BOLD responses while imagine speaking and imagine humming a melody. Therefore, we performed connectivity analysis only for these two clusters. When subsuming imagine speaking and imagine humming in a conjunction analysis, group contrasts revealed an increased correlation between the left area 44pd (cluster 1) and the left parietal operculum (OP1) as well as bilateral inferior parietal regions (left PFmc and right PGa) in control participants relative to AWS. In addition, control participants showed an increased correlation of the left area 44pv (cluster 4) with the right inferior parietal lobule including PGp and Pga, which is located on the angular gyrus, as well as an increased correlation with activity in the posterior cingulate gyrus (pCG). Fig. 5 illustrates these PPI results. The overlap of increased correlations in the right IPL/PGa is of particular interest. Group differences were evident for both seed regions in the IPL/PGa. All PPI results are reported in Table 5.

Furthermore, PPI yielded significant anticorrelations in control participants, which were missing in AWS. These negative correlations involved the left anterior middle temporal gyrus (aMTG) for both seed regions. Significant clusters in the left aMTG overlapped, as shown in Fig. 6. Additionally, left area 44pv was decoupled from the right premotor cortex in control participants.

3.4. Right posterior area 44 is likewise involved in imagery of speaking and humming in fluent speakers, but in AWS, activity for imagery of humming is smaller compared to activity for imagery of speaking

Speaking and humming are associated with an opposite lateralization of activity in frontal-motor areas. Speaking showed stronger

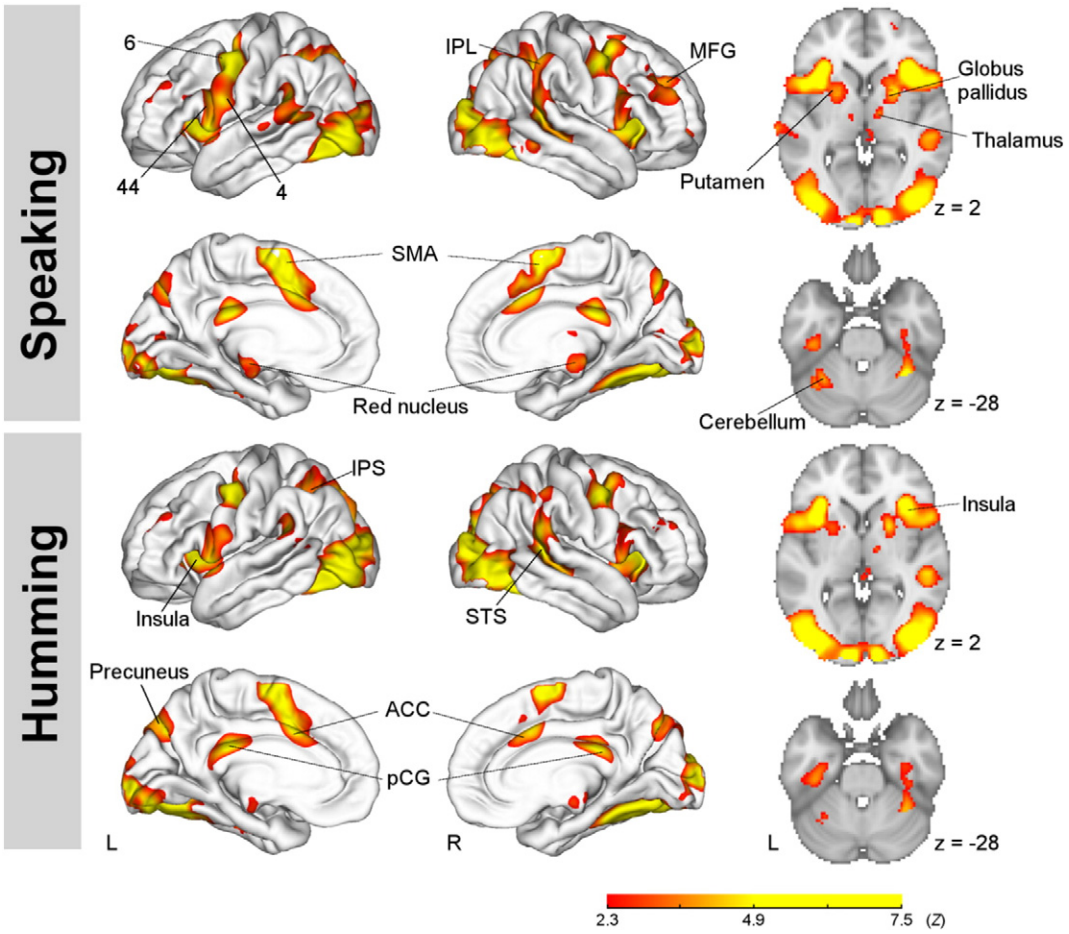

Fig. 3. Activation maps derived from a whole-brain analysis across all 32 participants are rendered on the surface of the brain. Similar networks were recruited during imagine speaking and imagine humming involving bilateral activations of the posterior inferior frontal gyrus (44), area 6, area 4, insula, operculum, supplementary motor area (SMA), anterior cingulate cortex (ACC), posterior cingulate gyrus (pCG), precuneus, inferior parietal lobule (IPL), the intraparietal sulcus (IPS), the superior temporal sulcus (STS), visual regions, the thalamus, and the red nucleus. Axial slices show bilateral activations of the insula, putamen, globus pallidus, thalamus, and cerebellum.

involvement of left frontal areas, whereas humming showed stronger activations of the right hemisphere (Callan et al., 2006; Jeffries et al., 2003; Riecker et al., 2000). From a behavioural point of view, it is important to note, that stuttering occurs when speaking but not when singing. Furthermore, stuttering is associated with a shift of speaking-related activity towards right frontal-motor areas (Belyk et al., 2015; Budde et al., 2014; Fox et al., 1996; Neef et al., 2015a). Here, left frontal area 44 showed a stronger involvement while imagine speaking, compared to imagine humming a melody. However, whether this pattern is reversed in the right hemisphere and whether stuttering is associated with a higher involvement of right area 44 is an open question. To date, no cross-functional co-activation-based parcellation of right area 44 has been published. For this reason, we determined right hemisphere homologue areas of cluster 1 and cluster 4 by physiological correlation analysis between the time courses of the left hemisphere clusters with the time course of all other voxels. Fig. 7 illustrates the seed regions for both analyses; the resulting functional connectivity emerged distinctively in the neighboring voxels of the seed region as well as in its right hemisphere homologue areas. Table 6 summarizes resulting correlations with these homologue areas ($Z > 10$, FWEC cluster-threshold). We applied this relatively high threshold to separate clusters and to achieve a comparable number of voxels in each of them. After thresholding, right cluster 1 included 154 voxels (1232 mm^3), and right cluster 4 included 155 voxels (1240 mm^3).

Statistical analyses were again performed on parameter estimates. To test variance between groups (control and AWS), and across hemispheres (left and right) and modes (speaking and humming), we calculated $2 \times 2 \times 2$ mixed-model ANCOVAs for the two posterior clusters. Fluency served as a covariate. ANCOVA of area 44pd yielded an effect of Group, $F(1,27) = 6.63$, $p = 0.015$, $\eta_p^2 = 0.186$, an effect of Mode, $F(1,27) = 17.12$, $p < 0.001$, $\eta_p^2 = 0.371$, an interaction of Hemisphere × Mode, $F(1,27) = 4.31$, $p = 0.047$, $\eta_p^2 = 0.129$, and an interaction of Group × Hemisphere × Mode, $F(1,27) = 6.95$, $p = 0.015$, $\eta_p^2 = 0.186$. Fluency was an influencing covariate, $F(1,29) = 4.90$, $p = 0.035$, $\eta_p^2 = 0.145$. To disentangle the three-way interaction with respect to the influence of mode, additional 2×2 ANCOVAs were calculated separately for each group. For controls, this analysis confirmed only the effect of Mode, $F(1,15) = 7.33$, $p = 0.016$, $\eta_p^2 = 0.328$ and the interaction of Hemisphere × Mode, $F(1,15) = 12.36$, $p = 0.003$, $\eta_p^2 = 0.452$. Fluency had no influence. Fig. 8 shows that in the right hemisphere of controls, the magnitude of parameter estimates is similar for speaking and humming. Thus, the interaction of Hemisphere × Mode is caused by the strong speaking-related signal increase in left area 44pd. For AWS, the analysis confirmed the effect of Mode, $F(1,13) = 12.21$, $p = 0.004$, $\eta_p^2 = 0.484$, but no interaction of Hemisphere × Mode. In AWS, fluency was an influencing covariate, $F(1,13) = 5.25$, $p = 0.039$, $\eta_p^2 = 0.288$. Fig. 8 shows that in AWS speaking-related activation is always higher than humming-induced activation, independent of hemisphere.

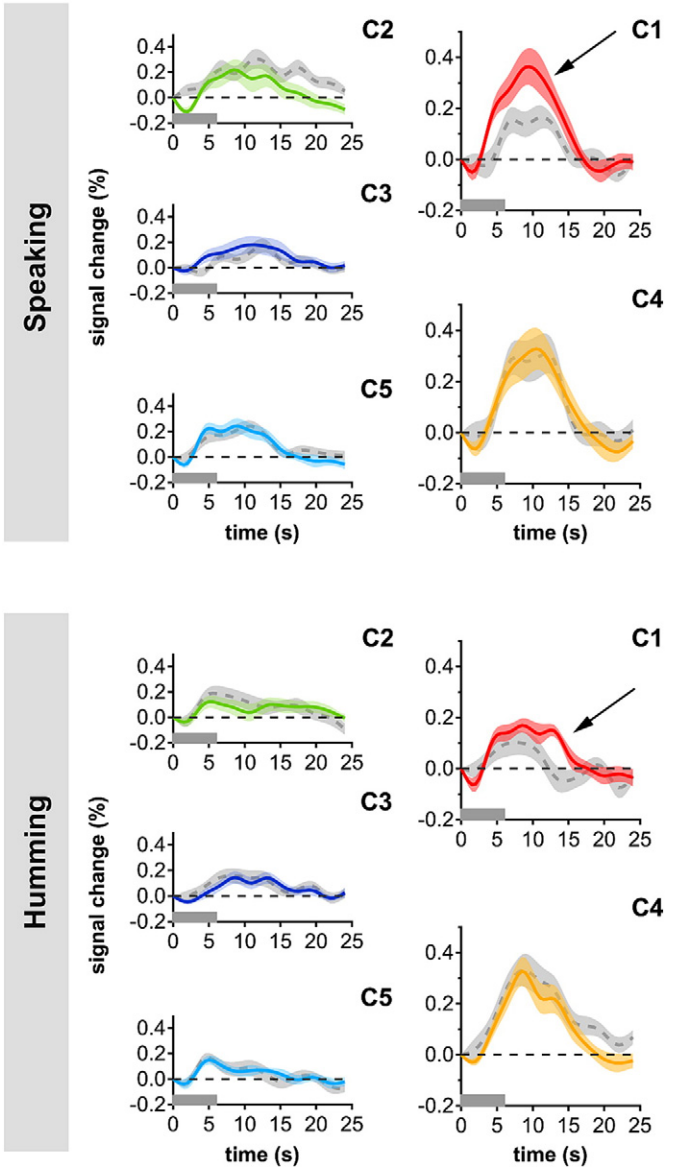

Fig. 4. Grand-average time courses of BOLD response separated for five functionally distinct clusters of left area 44. Grey lines represent AWS (n = 15), coloured lines represent controls (n = 17). Shaded areas indicate the standard error. Note the decreased speaking-related and humming-related activation in AWS in the posterior-dorsal cluster 1.

A 2 × 2 × 2 ANCOVA of area 44pv yielded only an interaction of Group × Hemisphere × Mode, $F(1,27) = 5.48$, $p = 0.026$, $\eta_p^2 = 0.159$, with a trending influence of fluency, $F(1,29) = 4.15$, $p = 0.051$, $\eta_p^2 = 0.125$. To disentangle this three-way interaction with respect to the influence of mode, additional 2 × 2 ANCOVAs were calculated separately for each group. In controls this analysis likewise confirmed an interaction of Hemisphere × Mode, $F(1,15) = 5.65$, $p = 0.031$, $\eta_p^2 = 0.274$, fluency had no influence. Fig. 8 illustrates this interaction, which is similar to the interaction already observed in cluster 1. Thus, controls showed a higher activation of left area 44pv when imagine speaking compared to imagine humming, but showed similar activation levels in the right hemisphere homologue. For AWS, the analysis settled an effect of Mode, $F(1,13) = 5.50$, $p = 0.036$, $\eta_p^2 = 0.297$, and a trending influence of fluency, $F(1,13) = 4.627$, $p = 0.051$, $\eta_p^2 = 0.263$, but no interaction of Hemisphere × Mode. Fig. 6 shows that speaking, compared to humming, induced higher activations in both posterior-ventral clusters of area 44 in AWS.

4. Discussion

Left Brodmann area 44, the posterior part of Broca's region, is subdivided into structurally and functionally distinct subregions. The aim of the present study was to determine the subregions that primarily contribute to the trait of stuttering by using a simple speech planning task and a vocal planning task. This focus is relevant because the left IFG is a prominent neuronal correlate of stuttering, but is coupled with various language-related as well as domain-general functions, ranging from linguistic operations such as hierarchical structure building, phonological processing and articulatory planning to action imagination, action sequencing, working memory processing, executive control, as well as aspects of music processing. Thus, a closer look at functionally distinct regions in area 44 and related networks that show particularly altered activations in AWS likewise improve neurobiological theories of stuttering as well as neuroanatomic theories of speech and language organization in general. To account for the fact that stuttering is associated with pronounced right hemisphere contributions, and to consider the bihemispheric involvement of area 44 in the currently applied tasks, we additionally extracted activations from right hemisphere homologue areas. Our discussion focuses on four main findings: (1) Stuttering was associated with a reduced activation of left area 44pd (cluster 1), a region that is associated with speech production, including phonological word processing, pitch processing, working memory processes, sequencing, motor planning, pseudoword learning, and action inhibition. (2) AWS showed a deficient fronto-parietal coupling when seeding in left area 44pd and left area 44pv, which was evident in control participants. (3) AWS showed a relatively increased BOLD response in right area 44pd while imagined speaking, but relatively reduced right hemisphere activations while they imagined humming a melody, with even altered brain functions for the preserved ability to sing. (4) Cluster-related time courses of the posterior subregions in area 44 showed delayed peak activations in the right hemisphere in both groups, suggesting a contribution of this region to the offset response of the task, which relates to the stopping of motor responses. The following sections provide a closer discussion of these results.

4.1. Left posterior areas 44

A previous co-activation based parcellation of area 44 suggested 5 functionally distinct subareas coupled in partially overlapping brain networks and associated with various cognitive functions (Clos et al., 2013). Here, applied motor imagery tasks induced positive BOLD responses in left area 44 with an anterior-to-posterior gradient showing that the largest activations occurred in the two posterior portions of left area 44. Peak of activation was similarly located in several studies. When participants imagined speaking a sub-lexical syllable, this induced the peak maximum at [x = −58, y = 6. z = 12] (Tian et al., 2016). The preparation to repeat a train of the syllable [ta] induced the peak maximum at [x = −57, y = 6, z = 9] (Brendel et al., 2010). These coordinates are closest to the centre of gravity of the posterior-ventral cluster 4 [x = −56, y = 8, z = 10] (Clos et al., 2013). The current data support the notion that the posterior portion of left area 44v is associated with action imagination, here, specifically in the auditory-to-motor domain. Imagine speaking and imagine humming include the planning and covert simulation of articulation, pitch modulation, rhythm production, and sequencing. Cognitive demands in terms of linguistic operations, hierarchical processing, or memory retrieval were comparably low in the used tasks in the current study. Speaking the months of the year is a highly automatized motor behaviour (Smith and Zelaznik, 2004). Singing or humming is based on this automatized speech motor coordination system (Kleber et al., 2010). Thus, our results are in line with the theory that an increasing degree of automation likely involves posterior regions of the left IFG (Badre, 2008; Jeon and Friederici, 2015; Uddén and Bahlmann, 2012).

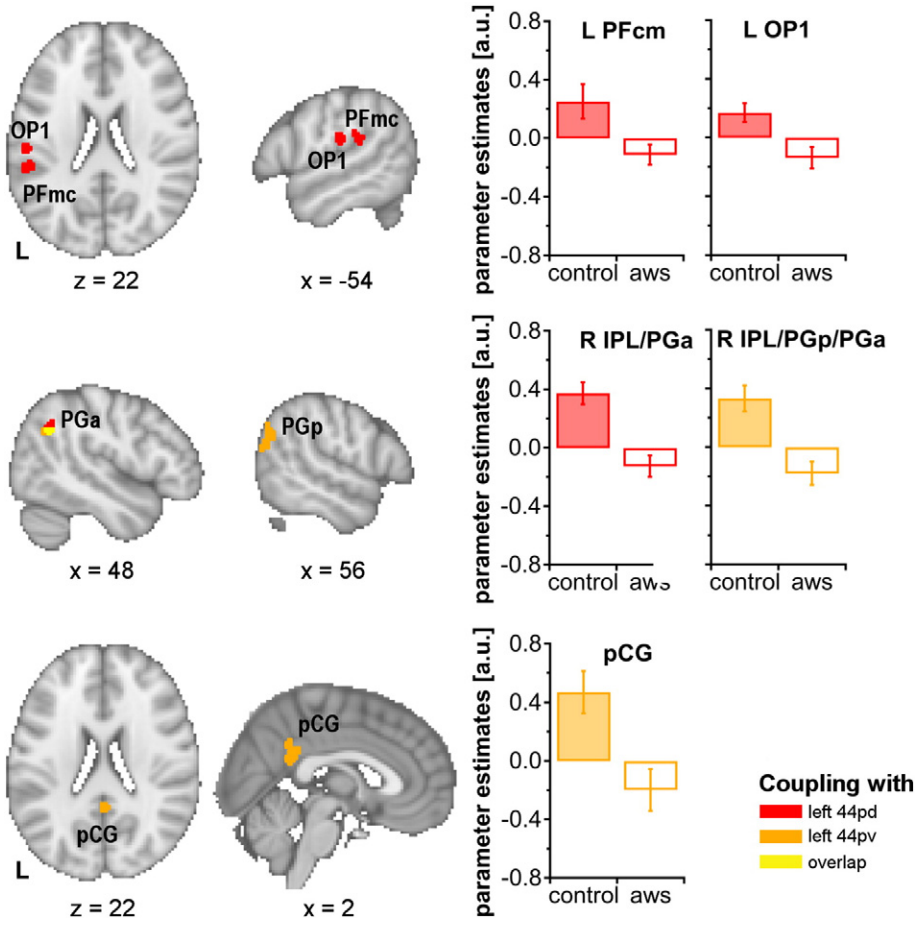

Fig. 5. PPI yielded increased functional coupling for control participants relative to AWS as shown in group contrast maps. Task-related activity of left area 44pd was more strongly correlated with the left parietal operculum (OP1), the left inferior parietal lobule (PFmc), and the right parietal lobule (PGa) in control participants compared to adults who stutter (AWS). Task-related activity of left 44pv showed stronger correlations with the right inferior parietal lobule (PGa, PGp) as well as the posterior cingulate gyrus (pCG) in control participants compared to AWS. *Z*-statistics were thresholded using clusters determined by $Z > 2.3$ and a (corrected) cluster significance threshold of $p = 0.05$, $k > 15$ (Worsley, 2001).

Interestingly, BOLD responses were larger in magnitude when participants imagined speaking the over-learned vocal sequence, compared to imagine humming the nonverbal tune of Mozart's "Eine kleine Nachtmusik" (Serenade No. 13 for strings in G major). The effect of mode was evident in posterior clusters 1 and 4 as well as in the two anterior clusters 2 and 5. Because covert responses cannot be measured, it is difficult to disentangle the causes of this effect of mode. Differences in timing and rhythm can contribute to such an effect (Brendel et al., 2010; Riecker et al., 2006) because of the missing preparation of sounds and syllables during imagine humming a melody that is not filled with words. The fact that the magnitude of the BOLD responses was the same in both groups in left area 44pv during imagining melody humming supports the assumption that both groups performed comparably well in the scanner (in terms of compliance).

Table 5
Group differences in effective connectivity of left area 44pd (cluster 1) and left area 44pv (cluster 4) subsuming imagery of speaking and humming in a conjunction analysis.

Region	Cytoa	x	y	z	Peak *Z*	Voxel
Cluster 1 speaking ∩ humming control > aws						
L parietal operculum	OP1	−54	−22	22	2.73	17
L inferior parietal lobule	PFcm	−54	−36	22	3.24	24
R inferior parietal lobule	PGa	48	−56	32	2.65	17
Cluster 1 speaking ∩ humming control < aws						
L anterior middle temporal gyrus		−58	0	−30	2.95	44
Cluster 4 speaking ∩ humming control > aws						
R inferior parietal lobule	PGp	54	−64	36	3.05	76
➢ R inferior parietal lobule	PGa	48	−58	30	2.6	
Posterior cingulate gyrus		0	−44	30	2.67	44
Cluster 4 speaking ∩ humming control < aws						
R premotor cortex	6	56	2	42	2.86	20
L anterior middle temporal gyrus		−54	−4	−34	2.83	17

Z-statistics were thresholded using clusters determined by $Z > 2.3$ and a (corrected) cluster significance threshold of $p = 0.05$, $k > 15$ (Worsley, 2001).

Stuttering was related to a decreased activity of posterior-dorsal cluster 1 in left area 44. The positive correlation between BOLD activity and stuttering frequency in an offline speech sample confirmes the role of this particular portion of left area 44 in stuttering. Because the applied task did not require overt speech production, but its covert simulation, this implies a neurophysiological burden of the trait of stuttering on speech planning related processes rather than articulatory related processes. A case study reported stuttering-associated activations in a single participant in the brain location studied here [x = −56, y = 8, z = 21] (Wymbs et al., 2013). A group study associated stuttering with reduced resting state functional connectivity in left area 44, 10 mm anterior to the locus of alteration in this study [x = −54, y = 18, z = 18] (Lu et al., 2012). Another group study reported decreased activations during sentence reading under normal and altered auditory feedback 6 mm posterior to the area considered here [x = −54, y = 2, z = 24] (Watkins et al., 2008) and labelled this coordinate with the ventral premotor cortex in accordance with the Harvard-Oxford Structural Atlas. The labels used in the current study were derived from the Juelich Histological Atlas (Eickhoff et al., 2005), which assigned the same coordinate to area 44 with a probability of 22%. Clearly, brain coordinates derived from MRI studies can only give an approximation, and labelling

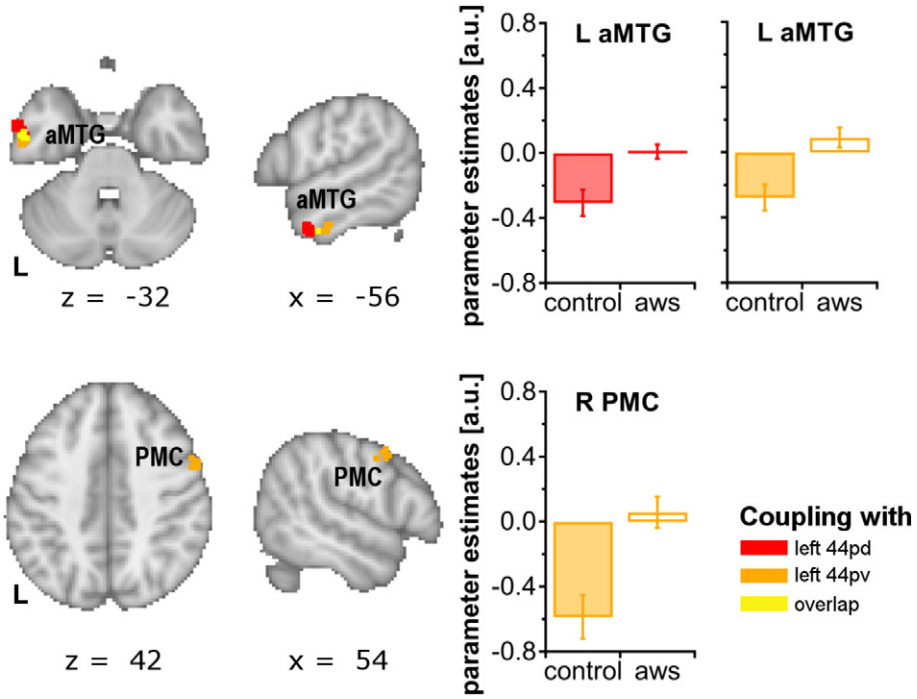

Fig. 6. PPI yielded anticorrelations in control participants relative to AWS as shown in group contrast maps. Task-related activity of left 44pd was negatively correlated with the left anterior middle temporal gyrus (aMTG) in control participants, compared to adults who stutter (AWS). Task-related activity of left 44pv showed negative correlations with the left aMTG as well as with the right premotor cortex (PMC) in control participants compared to AWS. *Z*-statistics were thresholded using clusters determined by $Z > 2.3$ and a (corrected) cluster significance threshold of $p = 0.05$, $k > 15$ (Worsley, 2001).

the underling structure results from probability maps aligned to a brain normalized across largely varying brains. To make matters even more challenging, individual data have usually a spatial resolution of $(3\ mm)^3$ or less and are interpolated due to motion correction and smoothing with 5 to 8 mm Gaussian filters. Irrespective of these spatial uncertainties, we agree with the assumption of most author's that left posterior area 44 is a locus where the intrinsic functional architecture of speech production is altered in stuttering (Beal et al., 2015; Chang et al., 2011; Kell et al., 2009; Lu et al., 2012; Watkins et al., 2008).

4.2. Left posterior areas 44 lacked the functional coupling with parietal areas in stuttering

During the tasks, posterior area 44 worked in connection with a large-scale network including the premotor cortex (area 6), anterior insula, SMA, frontal operculum, ventral primary motor cortex, middle frontal gyrus, inferior parietal lobule, putamen, globus pallidus, thalamus, and cerebellum (Fig. 3), structures associated with articulatory imagery (Tian et al., 2016). In the context of stuttering, our functional connectivity analysis of the present data highlights the significance of a left area 44pd-to-parietal coupling. The co-activation of left area 44pd with the left parietal operculum [$x = -54$, $y = -22$, $z = 22$] has been mapped to rhythm production (Konoike et al., 2012) and the activation of internal models that predict somatosensory outcome of the planned speech movement (Blakemore and Decety, 2001; Golfinopoulos et al., 2011; Tian et al., 2016). The co-activation of left area 44pd with the left area PFmc [$x = -54$, $y = -36$, $z = 22$], in the left Sylvian fissure, at the parieto-temporal boundary, has been mapped to verbal and tonal working memory (Koelsch et al., 2009), and has repeatedly been reported to be coactive during perception and covert production of speech (Hickok et al., 2008), and speech and music (Callan et al., 2006; Hickok et al., 2003). The reduced coactivation

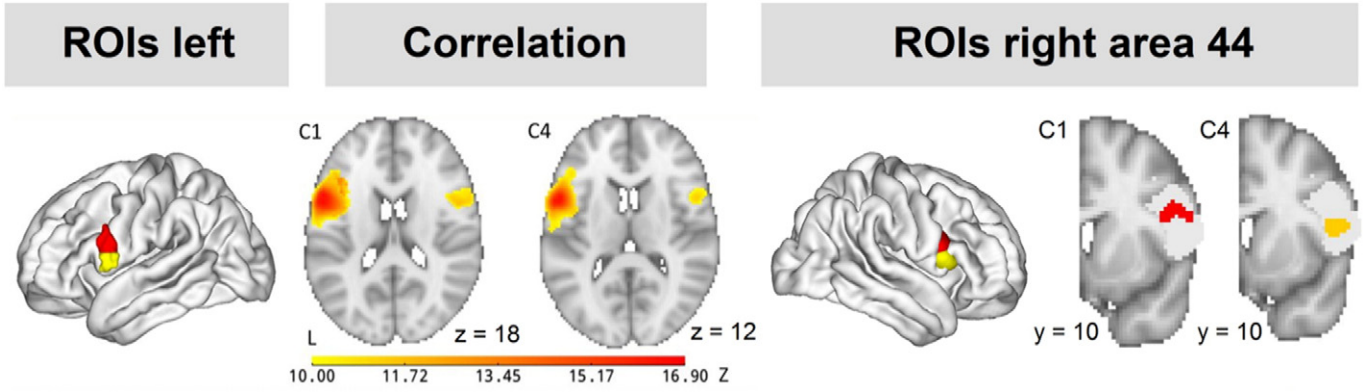

Fig. 7. Functional connectivity analyses revealed right hemisphere homologues of left hemisphere cluster 1 and cluster 4. Brain surface on the left shows left area 44pd (C1, red) and left area 44pv (C4, yellow). The two axial sections display the functional connectivity of left area 44pd (C1) and left area 44pv (C4) with neighboring voxels and their right hemisphere homologues. Extracted right hemisphere clusters are rendered on the surface of the right brain. The two coronal sections display clusters on the Juelich probability map of right area 44 (Amunts et al., 1999, 2004) in light-grey.

Table 6
Right IFG clusters evolving from functional connectivity analyses.

Cluster	Region	Cytoarchitectonic area	x	Y	z	Cluster size	Z-Max
C1	R IFG	Area 44 (46% overlap)	50	8	24	154	12.3
C4	R IFG	Area 44 (55% overlap)	54	10	12	155	11.6

of these fronto-parietal regions in stuttering might be caused by a deficient structural connectivity of the left superior longitudinal fasciculus as shown by diffusion MRI (Chang et al., 2011; Neef et al., 2015a).

In control participants left area 44pv activity showed an increased bilateral correlation with the inferior parietal lobule, which was more extended in the right hemisphere, stretching from PGa to PGp. These cytoarchitectonically distinct subdivisions of the inferior parietal lobule (Caspers et al., 2006, 2008) are coupled with overlapping, yet distinctive functional and structural networks (Uddin et al., 2010), thereby resampling a general principle of cortical areas. Human brain mapping studies suggest involvement in the preparation of potential motor responses (Thoenissen et al., 2002), control of motor sequences (Bengtsson et al., 2004), as well as the control and acquisition of motor and cognitive action sequences (Koechlin et al., 2002). In stuttering, bilateral activity in the inferior parietal lobes has been linked to increased fluency (Belyk et al., 2015; Budde et al., 2014; Neef et al., 2015a). Here, our data associated stuttering with a deficient functional interaction between left posterior area 44 and parietal areas. This finding suggests an insufficient neural implementation of internal representations of speech motor and tonal motor acts.

Human fMRI is unable to disentangle multilevel neural activity due to the anatomical complexity of each substrate, parallel loops, and recurrent dynamic interactions therein. On the basis of our data, we cannot be certain whether functional correlations were directly mediated by the superior longitudinal fasciculus/arcuate fasciculus via synaptic connections between left area 44 pd/44pv, or whether interconnections with different structures mediated physiological interactions, or whether our data only reflect a co-activation without any physiological interactions. However, the activity-related correlation that we observed was resampled by a functional connectivity analysis of resting state fMRI data (Buckner et al., 2011; Choi et al., 2012; Yeo et al., 2011). Seeding in left area 44pd (http://neurosynth.org/locations/-56_8_22_6/) or 44pv (http://neurosynth.org/locations/-56_8_10_6/) revealed a similarly strong functional correlation with the inferior parietal lobule in 1000 healthy participants (Fig. 9).

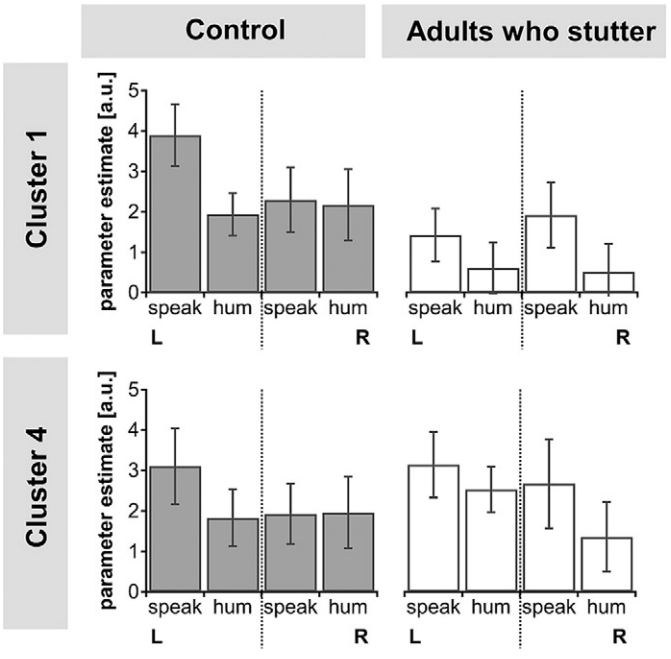

Fig. 8. Parameter estimates extracted from area 44pd (cluster 1) and area 44pv cluster 4) are displayed separately for group and hemisphere. Error bars indicate standard error.

The overlap of this network with the neural substrate of the control and acquisition of motor and cognitive action sequences (Abe and Hanakawa, 2009; Koechlin et al., 2002), and automatization of motor behaviour (Penhune and Doyon, 2002), allow us to speculate that insufficient automatization is a key element of the pathophysiology of stuttering. Speaking is a highly automatized motor action retrieving heavily overlearned motor sequences from motor memory. Fluency enhancing strategies rupture this automatized behaviour, and under high cognitive control demands, AWS render to speak more fluently by producing soft voice onsets without voice offsets or sound prolongations. The implementation of these strategies pushes prefrontal cortex activity into achieving the monitoring of unfamiliar sounding auditory goals. These strategies heavily involve the feedback control system. They require monitoring of self-generated performance and preparation of forthcoming sequential actions in an unaccustomed way. Training of such fluency-enhancing speech modes was associated with activations of area 47, in AWS (Kell et al., 2009), as well as in fluent speakers (Toyomura et al., 2015). The idea that automatization is deficient in stuttering is in addition supported by the observation that fluency-enhancing strategies have transient effects, and beneficial power vanishes with long-term practice (Euler et al., 2009). It is tempting to speculate that motor speech tasks with high control demands on the speech motor coordination system, and thus a stronger involvement of anterior prefrontal regions facilitate fluency, while the common speech mode employed in daily conversation relies on a system with a high degree of automaticity and is thus vulnerable to break-downs in individuals who stutter due to the weakness of left area 44.

4.3. Humming is special in stuttering

We employed imagery of humming as a control task because singing induces desirable fluency in AWS. Against our expectation, brain activation associated with imagery of humming was irregular in AWS. Their left hemisphere activation in area 44pd was reduced compared to activity observed in fluent speakers. Furthermore, right hemisphere homologue area 44pd showed likewise smaller magnitudes for imagery of humming, compared to imagery of speaking in AWS. In contrast, fluent speakers showed comparably large magnitudes of activation in both tasks and in both posterior clusters in the right hemisphere. The contradictions are twofold. Firstly, typical behaviour, specifically regular singing (Andrews et al., 1982), was associated with locally reduced activity in posterior area 44. Secondly, the frequently reported pattern of an increased activation of the right hemisphere in AWS (Belyk et al., 2015; Budde et al., 2014) did not occur while imagery of humming in the current data. These data suggest that in AWS, core neurofunctional correlates of stuttering showed an aberrant activation during covert humming. Previously observed right hemisphere overactivations of the IFG possibly only come into play during actual speaking and actual humming, but not during motor imagery. This suggestion is supported by the theory that right hemisphere IFG activity mediates auditory and somatosensory feedback control (Golfinopoulos et al., 2011; Guenther and Hickok, 2015; Tourville et al., 2008), which is supposed to be irregular in AWS too (Cai et al., 2012). However, feedback related processes have not been addressed in the current motor imagery tasks. Future research is needed to further elucidate physiological mechanisms of fluent vocal productions and to disentangle neuronal principles that render fluency while singing, which is not achieved while speaking.

4.4. Distinctive stopping response in the right hemisphere – a cause of stuttering?

Right hemisphere activity has been intimately connected with the neuroanatomy of stuttering since the first imaging studies in this field

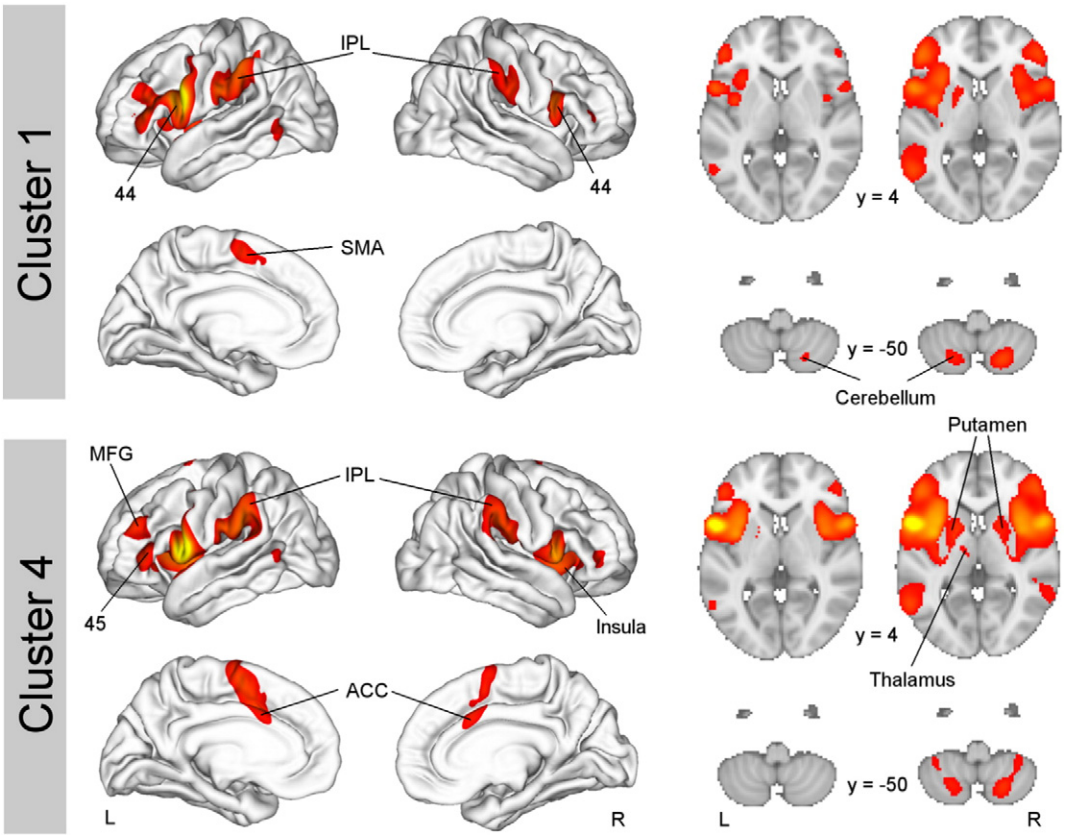

Fig. 9. Resting-state functional connectivity of the posterior subregions of left area 44. Displayed are images of two resting-state functional connectivity analyses for seed regions in the left posterior-dorsal area 44 (Cluster 1) with the center of gravity at [x = −56, y = 8, z = 22] and in the left posterior-ventral area 44 (Cluster 4) with the center of gravity at [x = −56, y = 8, z = 10]. The analysis was calculated across a sample of 1000 healthy subjects via Neurosynth (http://neurosynth.org). The red-to-yellow colour gradient indicates correlation coefficients ranging from r = 0.2 (red) to r = 0.5 (yellow) for the first three columns. Axial slices of the most right column display the expansion of the network bilateral fronto-parieto-insular network towards subcortical structures (putamen, thalamus and cerebellum) when lowering the threshold to r = 0.1.

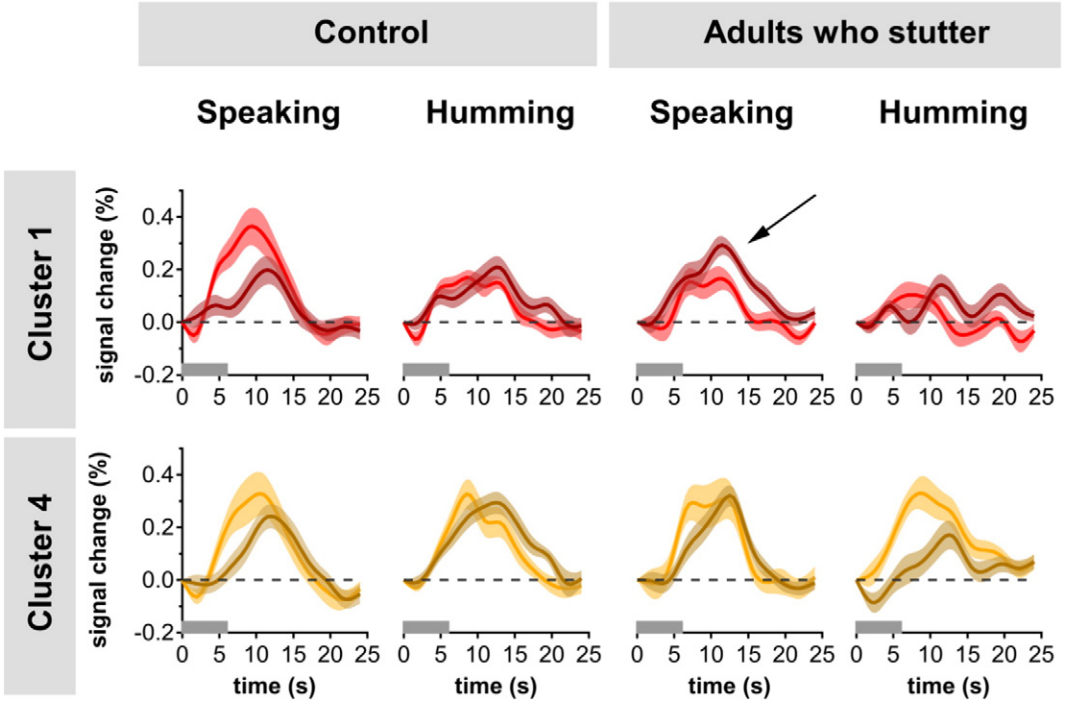

Fig. 10. Grand-average time courses of BOLD response separated for mode and site. Pale colours display left hemisphere responses, dark colours represent right hemisphere responses. Shaded areas indicate the standard error. The grey filled square in the right corner of each plot indicates the 6-second time duration of the task.

(Braun et al., 1997; Fox et al., 1996). In the right hemisphere, overactivations have been reported for the primary motor cortex in co-activation with the premotor cortex, the pre-supplementary motor area, the supplementary motor area, the inferior frontal gyrus (IFG), the insula, and the frontal and the rolandic operculum, a circuit that is associated with the regulation of motor functions (Belyk et al., 2015; Budde et al., 2014). It remains an open question as to whether the strong involvement of the right hemisphere motor areas to the speech production of those who stutter is a cause of stuttering, a result of a left hemisphere structural and functional connectivity deficit (Chang et al., 2011; Chang et al., 2015; Cieslik et al., 2013; Cykowski et al., 2010; Kell et al., 2009; Kronfeld-Duenias et al., 2014; Neef et al., 2015b; Neef et al., 2015a; Salmelin et al., 2000; Sommer et al., 2001; Vanhoutte et al., 2016; Watkins et al., 2008), or whether it reflects compensatory mechanisms (Braun et al., 1997; Kell et al., 2009; Kikuchi et al., 2011; Neef et al., 2011a; Preibisch et al., 2003; Yang et al., 2016).

The current results linked stuttering with altered activations of the right hemisphere. First, while imagine speaking, right hemisphere activity was increased in AWS, compared to left hemisphere activity. This is consistent with previous reports. Second, a closer look at the time courses clearly revealed consistently delayed peak latencies of right hemisphere responses, compared to left hemisphere responses in both groups (Fig. 10). We speculate that the delayed peaks correspond to the offset response rather than to the execution of the task itself. Participants were asked to imagine speaking or humming until a stop signal occurred, which happened after 6 s. Because the responses had a biphasic shape, especially in cluster 1, we think it is plausible to assume that the waveform of the inherently slow hemodynamic response reflects interference between executing the task and stopping the task. We provide support for this assumption by reporting the results of an additional group independent component analysis (ICA) (Calhoun et al., 2001; Calhoun and Adali, 2006; Eichele et al., 2008) in the supplementary material. This ICA revealed two distinctive independent components that involved the right posterior area 44. One independent component was related to the process of vocal motor imagery, the other independent component was related to the imagery offset, and thus, to the stopping of the motor imagery (Fig. 11).

In addition, our interpretation is supported by the theory that right ventrolateral premotor cortex is, among other functions (Aron et al., 2014), involved in motor inhibition, where control is engaged to stop or override manual motor responses (Levy and Wagner, 2011; Majid et al., 2013). Besides the inhibition of manual responses, the inhibition of speech response is likewise associated with increased activations in the right IFG pars opercularis extending to the anterior insular cortex (Xue et al., 2008). A huge body of imaging studies link the right IFG to inhibitory motor control (Aron et al., 2014) with the most compelling evidence coming from a study involving transcranial magnetic stimulation. A deactivation of the right posterior area 44 interfered with the ability to stop an initiated action (Chambers et al., 2006). Similarly to the left IFG, the right IFG is subdivided into cytoarchitectonically and functionally distinct subregions (Amunts et al., 1999, 2004). A recent co-activation based parcellation across the right IFG pars opercularis and pars triangularis considered stop-signal task-evoked hemodynamic responses. Two distinct clusters were generated, a posterior-dorsal cluster and a posterior-ventral cluster both occupying the pars opercularis of the right IFG (Cai et al., 2014). Thus, activation in pars opercularis is more likely to correspond to inhibition than pars triangularis or orbitalis (Aron et al., 2014), which supports our interpretation.

In the current study, the magnitude of the offset-response, which is related to the act of stopping a motor response was not larger in males who stutter compared to fluent speakers in right area 44. However, in comparison to the left hemisphere activation while imagine speaking, the right hemisphere response was relatively strong. One might argue that the increased stopping-related activity interacts with the initiation and forthcoming of desired speech movements as suggested by Xue et al. (2008). A recent connectivity analysis revealed a positive correlation between stuttering severity and resting-state functional connectivity between the right lobule VI of the cerebellum and the right IFG pars triangularis (Yang et al., 2016). The authors likewise suggest a role of the right IFG for the inhibition of speech. However, the authors interpret their results in the context of a compensatory role of the right prefrontal cortex. Increased confidence in the role of right inferior frontal activity in stuttering could be achieved through (a) greater anatomical precision that could be improved due to ultra-higher resolution fMRI

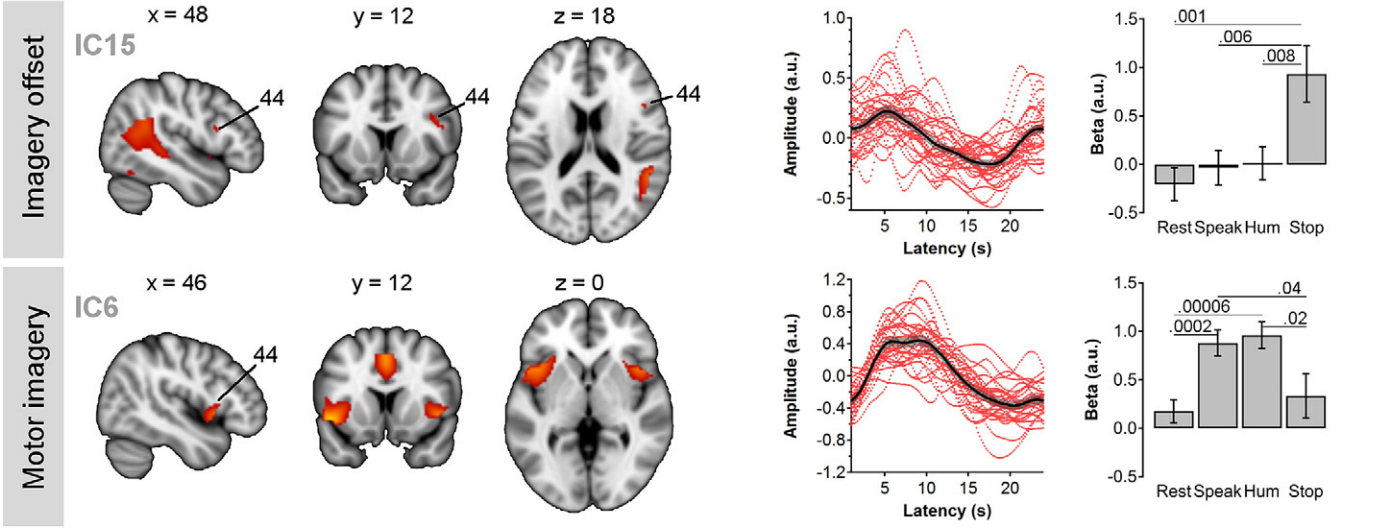

Fig. 11. Group ICA revealed independent components for stopping the motor response (IC15) and imagery of speaking and humming (IC6). Component maps are rendered onto the MNI template at representative sagittal (left), coronal (center), and axial (right) slices; coordinates in mm are given at the top. The maps are shown in neurological convention (right hemisphere is on the right). Hemodynamic responses are plotted within the respective component as estimated via deconvolution from 1 to 24 s after stimulus onset (IC15 - stop signal, IC6 – imaginary of speaking or humming signal). The group average across all participants is plotted as a solid line; the shaded area indicates 95% confidence interval, and dots represent all individual estimates. Bar plots display β-estimates ($\pm$SEM) as revealed by component specific GLMs. Two-way ANCOVAs with group as between-subjects factor and condition as within-subjects factor revealed significant effects of condition (IC15 - $F(1,58) = 8.25$, $p = 0.0.006$; IC6 - $F(1,58) = 4.91$, $p = 0.0.031$). For details, see Supplementary material. p-Values of post-hoc t-tests indicate psycho-physiological relations, Accordingly, IC15 was associate to stopping the motor imagery task whereas IC6 was associated to actual vocal motor imagery.

(Heidemann et al., 2010; Huber et al., 2015); (b) focusing on brain networks rather than the IFG alone (Wiecki and Frank, 2013); (c) addressing other functional criteria for inhibition, such as TMS signatures of motor suppression (Neef et al., 2015b; Neef et al., 2011a; Neef et al., 2011b; Stinear et al., 2009), or studying movement-related alpha/beta desynchronization of the sensorimotor cortex or the basal ganglia (Etchell et al., 2015; Swann et al., 2009).

Recent computational models focusing on networks rather than the IFC activity alone suggest a global response suppression mechanism along a subthalamic nucleus-rIFG-basal ganglia hyperdirect pathway (Wiecki and Frank, 2013). This pathway is assumed to provide a global dynamic regulation by transiently suppressing competing candidate motor responses when there is conflict between alternative actions (Frank, 2006). In the context of stuttering, this model supports the dopaminergic hypothesis (Alm, 2004; Wu et al., 1997), postulating a hyperdopaminergic state as the cause of stuttering. This hypothesis is supported by studies on neurogenic stuttering. Stuttering was for instance aggravated by deep brain stimulation of the subthalamic nucleus (Toft and Dietrichs, 2011; Tsuboi et al., 2015); however, other studies report a remediating effect (Walker et al., 2009). A dysregulation of tonic dopamine is likewise associated with stuttering in both cases, acquired stuttering (Tykalová et al., 2015) or persistent develop mental stuttering (Wu et al., 1995, 1997). Moreover, pharmacological intervention showed an alleviation of persistent developmental stuttering followed by the administration of dopamine receptor antagonists (Maguire et al., 2010; Maguire et al., 2004). Future studies are necessary to address the question whether stuttering results from an increased contribution of brain circuits involved in the control of stopping motor responses.

5. Conclusion

In summary, the current study provides greater anatomical precision with regard to the role of Broca's area in stuttering. Focusing on left and right area 44, a cytoarchitectonically defined region occupying the posterior portion of the pars opercularis of the IFG, we converged two main principles: First, left posterior-dorsal area 44 is a core neuroanatomical correlate of impaired speech motor preparation in stuttering, which is even evident during the planning of humming. Second, we speculate that right posterior-dorsal area 44 is mainly involved in the control of motor inhibition. For this reason we hypothesize that stuttering could be caused by an amplified inhibitory activity of the hyperdirect rIFG-STN-BG pathway. We are looking forward to future studies addressing this question by employing sophisticated methods. Eventually, our results may pave the way to targeted transcranial stimulation protocols for treatment by inhibiting right area 44 and exciting left area 44.

Authors contributions

N.E.N. and M.S. conceived and designed the experiment; C.B. performed the experiment; N.E.N analyzed the data; A.W. contributed unpublished visualization tools; N.E.N. wrote the paper, all authors commented on the paper.

Acknowledgments

This work was funded by the Dorothea Schlözer Fellowship Programme of the University of Göttingen (to N.E.N.), and by the Deutsche Forschungsgemeinschaft (NE 1841/1-1 to N.E.N; and SO 429/2-2; SO 429/4-1 to M.S. We are thankful to Kristina Anders for the analysis of the speech samples, Carsten Schmidt-Samoa for adjusting the program for stimulus presentation, Peter Dechent for his recommendations regarding the MR sequences, Ilona Pfahlert and Britta Perl for their help with MRI data aquisition.

Appendix A. Supplementary data

Supplementary data to this article can be found online at http://dx.doi.org/10.1016/j.neuroimage.2016.08.030.

References

Abe, M., Hanakawa, T., 2009. Functional coupling underlying motor and cognitive functions of the dorsal premotor cortex. Behav. Brain Res. 198 (1), 13–23. http://dx.doi.org/10.1016/j.bbr.2008.10.046.

Aboitiz, F., Garćia, V.R., 1997. The evolutionary origin of the language areas in the human brain. A neuroanatomical perspective. Brain Res. Rev. 25 (3), 381–396. http://dx.doi.org/10.1016/S0165-0173(97)00053-2.

Alm, P.A., 2004. Stuttering and the basal ganglia circuits: a critical review of possible relations. J. Commun. Disord. 37 (4), 325–369. http://dx.doi.org/10.1016/j.jcomdis.2004.03.001.

Amunts, K., Schleicher, A., Bürgel, U., Mohlberg, H., Uylings, H.B.M., Zilles, K., 1999. Broca's region revisited: cytoarchitecture and intersubject variability. J. Comp. Neurol. 412 (2), 319–341. http://dx.doi.org/10.1002/(SICI)1096-9861(19990920)412:2<319::AID-CNE10>3.0.CO;2-7.

Amunts, K., Weiss, P.H., Mohlberg, H., Pieperhoff, P., Eickhoff, S., Gurd, J.M., ... Zilles, K., 2004. Analysis of neural mechanisms underlying verbal fluency in cytoarchitectonically defined stereotaxic space—the roles of Brodmann areas 44 and 45. NeuroImage 22 (1), 42–56. http://dx.doi.org/10.1016/j.neuroimage.2003.12.031.

Amunts, K., Lenzen, M., Friederici, A.D., Schleicher, A., Morosan, P., Palomero-Gallagher, N., Zilles, K., 2010. Broca's region: novel organizational principles and multiple receptor mapping. PLoS Biol. 8 (9), e1000489. http://dx.doi.org/10.1371/journal.pbio.1000489.

Andersson, J.L.R., Jenkinson, M., Smith, S., 2010. Non-Linear Registration, Aka Spatial Normalisation. FMRIB Analysis Group Technical Reports.

Andrews, G., Howie, P.M., Dozsa, M., Guitar, B.E., 1982. Stuttering: speech pattern characteristics under fluency-inducing conditions. J. Speech Lang. Hear. Res. 25 (2), 208. http://dx.doi.org/10.1044/jshr.2502.208.

Anwander, A., Tittgemeyer, M., von Cramon, D., Friederici, A.D., Knösche, T.R., 2007. Connectivity-based parcellation of Broca's area. Cereb. Cortex 17 (4), 816–825. http://dx.doi.org/10.1093/cercor/bhk034.

Aron, A.R., Robbins, T.W., Poldrack, R.A., 2014. Inhibition and the right inferior frontal cortex: one decade on. Trends Cogn. Sci. 18 (4), 177–185. http://dx.doi.org/10.1016/j.tics.2013.12.003.

Badre, D., 2008. Cognitive control, hierarchy, and the rostro–caudal organization of the frontal lobes. Trends Cogn. Sci. 12 (5), 193–200. http://dx.doi.org/10.1016/j.tics.2008.02.004.

Beal, D.S., Gracco, V.L., Brettschneider, J., Kroll, R.M., De Nil, L.F., 2013. A voxel-based morphometry (VBM) analysis of regional grey and white matter volume abnormalities within the speech production network of children who stutter. Cortex 49 (8), 2151–2161. http://dx.doi.org/10.1016/j.cortex.2012.08.013.

Beal, D.S., Lerch, J.P., Cameron, B., Henderson, R., Gracco, V.L., De Nil, L., 2015. The trajectory of gray matter development in Broca's area is abnormal in people who stutter. Front. Hum. Neurosci. 9, 89. http://dx.doi.org/10.3389/fnhum.2015.00089.

Belyk, M., Kraft, S.J., Brown, S., 2015. Stuttering as a trait or state – an ALE meta-analysis of neuroimaging studies. Eur. J. Neurosci. 41 (2), 275–284. http://dx.doi.org/10.1111/ejn.12765.

Bengtsson, S.L., Ehrsson, H.H., Forssberg, H., Ullén, F., 2004. Dissociating brain regions controlling the temporal and ordinal structure of learned movement sequences. Eur. J. Neurosci. 19 (9), 2591–2602. http://dx.doi.org/10.1111/j.0953-816X.2004.03269.x.

Blakemore, S.-J., Decety, J., 2001. From the perception of action to the understanding of intention. Nat. Rev. Neurosci. 2 (8), 561–567. http://dx.doi.org/10.1038/35086023.

Bloodstein, O., Ratner, N.B., 2008. A Handbook on Stuttering. 6th ed. Delmar Learning, Clifton Park, NY.

Bohland, J.W., Guenther, F.H., 2006. An fMRI investigation of syllable sequence production. NeuroImage 32 (2), 821–841. http://dx.doi.org/10.1016/j.neuroimage.2006.04.173.

Bohland, J.W., Bullock, D., Guenther, F.H., 2009. Neural representations and mechanisms for the performance of simple speech sequences. J. Cogn. Neurosci. 22 (7), 1504–1529. http://dx.doi.org/10.1162/jocn.2009.21306.

Braun, A.R., Varga, M., Stager, S., Schulz, G., Selbie, S., Maisog, J.M., ... Ludlow, C.L., 1997. Altered patterns of cerebral activity during speech and language production in developmental stuttering. An H2(15)O positron emission tomography study. Brain 120 (5), 761–784. http://dx.doi.org/10.1093/brain/120.5.761.

Brendel, B., Hertrich, I., Erb, M., Lindner, A., Riecker, A., Grodd, W., Ackermann, H., 2010. The contribution of mesiofrontal cortex to the preparation and execution of repetitive syllable productions: an fMRI study. NeuroImage 50 (3), 1219–1230. http://dx.doi.org/10.1016/j.neuroimage.2010.01.039.

Brodmann, K., 1909. Vergleichende Lokalisationslehre der Grobhirnrinde in ihren Prinzipien dargestellt auf Grund des Zellenbaues. Barth JA, Leipzig.

Buchsbaum, B.R., Olsen, R.K., Koch, P., Berman, K.F., 2005. Human dorsal and ventral auditory streams Subserve rehearsal-based and echoic processes during verbal working memory. Neuron 48 (4), 687–697. http://dx.doi.org/10.1016/j.neuron.2005.09.029.

Buckner, R.L., Krienen, F.M., Castellanos, A., Diaz, J.C., Yeo, B.T.T., 2011. The organization of the human cerebellum estimated by intrinsic functional connectivity. J. Neurophysiol. 106 (5), 2322–2345. http://dx.doi.org/10.1152/jn.00339.2011.

Budde, K.S., Barron, D.S., Fox, P.T., 2014. Stuttering, induced fluency, and natural fluency: a hierarchical series of activation likelihood estimation meta-analyses. Brain Lang. 139, 99–107. http://dx.doi.org/10.1016/j.bandl.2014.10.002.

Bütfering, C., 2015. Geschlechtsspezifische Unterschiede sprechassoziierter Gehirnaktivität bei stotternden Menschen - Eine klinische Studie mittels funktioneller Magnetresonanztomographie (Dissertation). Georg-August-Universität, Göttingen.
Cai, S., Beal, D.S., Ghosh, S.S., Tiede, M.K., Guenther, F.H., Perkell, J.S., 2012. Weak responses to auditory feedback perturbation during articulation in persons who stutter: evidence for abnormal auditory-motor transformation. PLoS One 7 (7), e41830. http://dx.doi.org/10.1371/journal.pone.0041830.
Cai, W., Ryali, S., Chen, T., Li, C.-S.R., Menon, V., 2014. Dissociable roles of right inferior frontal cortex and anterior insula in inhibitory control: evidence from intrinsic and task-related functional parcellation, connectivity, and response profile analyses across multiple datasets. J. Neurosci. 34 (44), 14652–14667. http://dx.doi.org/10.1523/JNEUROSCI.3048-14.2014.
Calhoun, V.D., Adali, T., 2006. Unmixing fMRI with independent component analysis. IEEE Eng. Med. Biol. Mag. 25 (2), 79–90. http://dx.doi.org/10.1109/MEMB.2006.1607672.
Calhoun, V.D., Adali, T., Pearlson, G.D., Pekar, J.J., 2001. A method for making group inferences from functional MRI data using independent component analysis. Hum. Brain Mapp. 14 (3), 140–151. http://dx.doi.org/10.1002/hbm.1048.
Callan, D.E., Tsytsarev, V., Hanakawa, T., Callan, A.M., Katsuhara, M., Fukuyama, H., Turner, R., 2006. Song and speech: brain regions involved with perception and covert production. NeuroImage 31 (3), 1327–1342. http://dx.doi.org/10.1016/j.neuroimage.2006.01.036.
Caspers, S., Geyer, S., Schleicher, A., Mohlberg, H., Amunts, K., Zilles, K., 2006. The human inferior parietal cortex: cytoarchitectonic parcellation and interindividual variability. NeuroImage 33 (2), 430–448. http://dx.doi.org/10.1016/j.neuroimage.2006.06.054.
Caspers, S., Eickhoff, S.B., Geyer, S., Scheperjans, F., Mohlberg, H., Zilles, K., Amunts, K., 2008. The human inferior parietal lobule in stereotaxic space. Brain Struct. Funct. 212 (6), 481–495. http://dx.doi.org/10.1007/s00429-008-0195-z.
Chambers, C.D., Bellgrove, M.A., Stokes, M.G., Henderson, T.R., Garavan, H., Robertson, I.H., ... Mattingley, J.B., 2006. Executive "brake failure" following deactivation of human frontal lobe. J. Cogn. Neurosci. 18 (3), 444–455. http://dx.doi.org/10.1162/089892906775990606.
Chang, S.E., Erickson, K.I., Ambrose, N.G., Hasegawa-Johnson, M.A., Ludlow, C.L., 2008. Brain anatomy differences in childhood stuttering. NeuroImage 39 (3), 1333. http://dx.doi.org/10.1016/j.neuroimage.2007.09.067.
Chang, S.E., Horwitz, B., Ostuni, J., Reynolds, R., Ludlow, C.L., 2011. Evidence of left inferior frontal–premotor structural and functional connectivity deficits in adults who stutter. Cereb. Cortex 21 (11), 2507–2518. http://dx.doi.org/10.1093/cercor/bhr028.
Chang, S.E., Zhu, D.C., Choo, A.L., Angstadt, M., 2015. White matter neuroanatomical differences in young children who stutter. Brain 138 (3), 694–711. http://dx.doi.org/10.1093/brain/awu400.
Choi, E.Y., Yeo, B.T.T., Buckner, R.L., 2012. The organization of the human striatum estimated by intrinsic functional connectivity. J. Neurophysiol. 108 (8), 2242–2263. http://dx.doi.org/10.1152/jn.00270.2012.
Cieslik, E.C., Zilles, K., Caspers, S., Roski, C., Kellermann, T.S., Jakobs, O., ... Eickhoff, S.B., 2013. Is there "one" DLPFC in cognitive action control? Evidence for heterogeneity from co-activation-based parcellation. Cereb. Cortex 23 (11), 2677–2689. http://dx.doi.org/10.1093/cercor/bhs256.
Clos, M., Amunts, K., Laird, A.R., Fox, P.T., Eickhoff, S.B., 2013. Tackling the multifunctional nature of Broca's region meta-analytically: co-activation-based parcellation of area 44. NeuroImage 83, 174–188. http://dx.doi.org/10.1016/j.neuroimage.2013.06.041.
Cykowski, M.D., Fox, P.T., Ingham, R.J., Ingham, J.C., Robin, D.A., 2010. A study of the reproducibility and etiology of diffusion anisotropy differences in developmental stuttering: a potential role for impaired myelination. NeuroImage 52 (4), 1495–1504. http://dx.doi.org/10.1016/j.neuroimage.2010.05.011.
Desikan, R.S., Ségonne, F., Fischl, B., Quinn, B.T., Dickerson, B.C., Blacker, D., ... Killiany, R.J., 2006. An automated labeling system for subdividing the human cerebral cortex on MRI scans into gyral based regions of interest. NeuroImage 31 (3), 968–980. http://dx.doi.org/10.1016/j.neuroimage.2006.01.021.
Eichele, T., Debener, S., Calhoun, V.D., Specht, K., Engel, A.K., Hugdahl, K., ... Ullsperger, M., 2008. Prediction of human errors by maladaptive changes in event-related brain networks. Proc. Natl. Acad. Sci. 105 (16), 6173–6178. http://dx.doi.org/10.1073/pnas.0708965105.
Eickhoff, S.B., Stephan, K.E., Mohlberg, H., Grefkes, C., Fink, G.R., Amunts, K., Zilles, K., 2005. A new SPM toolbox for combining probabilistic cytoarchitectonic maps and functional imaging data. NeuroImage 25 (4), 1325–1335. http://dx.doi.org/10.1016/j.neuroimage.2004.12.034.
Eickhoff, S.B., Heim, S., Zilles, K., Amunts, K., 2009. A systems perspective on the effective connectivity of overt speech production. Philos. Trans. R. Soc. A Math. Phys. Eng. Sci. 367 (1896), 2399–2421. http://dx.doi.org/10.1098/rsta.2008.0287.
Etchell, A.C., Johnson, B.W., Sowman, P.F., 2015. Beta oscillations, timing, and stuttering. Front. Hum. Neurosci. 8, 1036. http://dx.doi.org/10.3389/fnhum.2014.01036.
Euler, H.A., Gudenberg, A.W.v., Jung, K., Neumann, K., 2009. Computergestützte Therapie bei Redeflussstörungen: Die langfristige Wirksamkeit der Kasseler Stottertherapie (KST). Sprache Stimme Gehör. 33(4) pp. 193–202. http://dx.doi.org/10.1055/s-0029-1242747.
Evans, A.C., Janke, A.L., Collins, D.L., Baillet, S., 2012. Brain templates and atlases. NeuroImage 62 (2), 911–922. http://dx.doi.org/10.1016/j.neuroimage.2012.01.024.
Fiebach, C.j., Schlesewsky, M., Lohmann, G., von Cramon, D.y., Friederici, A.d., 2005. Revisiting the role of Broca's area in sentence processing: syntactic integration versus syntactic working memory. Hum. Brain Mapp. 24 (2), 79–91. http://dx.doi.org/10.1002/hbm.20070.
Flinker, A., Korzeniewska, A., Shestyuk, A.Y., Franaszczuk, P.J., Dronkers, N.F., Knight, R.T., Crone, N.E., 2015. Redefining the role of Broca's area in speech. Proc. Natl. Acad. Sci. 112 (9), 2871–2875. http://dx.doi.org/10.1073/pnas.1414491112.
Fox, P.T., Ingham, R.J., Ingham, J.C., Hirsch, T.B., Downs, J.H., Martin, C., ... Lancaster, J.L., 1996. A PET study of the neural systems of stuttering. Nature 382 (6587), 158–162. http://dx.doi.org/10.1038/382158a0.
Frank, M.J., 2006. Hold your horses: a dynamic computational role for the subthalamic nucleus in decision making. Neural Netw. 19 (8), 1120–1136. http://dx.doi.org/10.1016/j.neunet.2006.03.006.
Friederici, A.D., 2011. The brain basis of language processing: from structure to function. Physiol. Rev. 91 (4), 1357–1392. http://dx.doi.org/10.1152/physrev.00006.2011.
Friston, K.J., Buechel, C., Fink, G.R., Morris, J., Rolls, E., Dolan, R.J., 1997. Psychophysiological and modulatory interactions in neuroimaging. NeuroImage 6 (3), 218–229. http://dx.doi.org/10.1006/nimg.1997.0291.
Geschwind, D.H., Miller, B.L., DeCarli, C., Carmelli, D., 2002. Heritability of lobar brain volumes in twins supports genetic models of cerebral laterality and handedness. Proc. Natl. Acad. Sci. 99 (5), 3176–3181. http://dx.doi.org/10.1073/pnas.052494999.
Golfinopoulos, E., Tourville, J.A., Bohland, J.W., Ghosh, S.S., Nieto-Castanon, A., Guenther, F.H., 2011. fMRI investigation of unexpected somatosensory feedback perturbation during speech. NeuroImage 55 (3), 1324–1338. http://dx.doi.org/10.1016/j.neuroimage.2010.12.065.
Guenther, F.H., Hickok, G., 2015. Chapter 9 - role of the auditory system in speech production. In: Aminoff, M.J., Boller, F., Swaab, D.F. (Eds.), Handbook of Clinical Neurology Vol. 129. Elsevier, pp. 161–175.
Gunji, A., Ishii, R., Chau, W., Kakigi, R., Pantev, C., 2007. Rhythmic brain activities related to singing in humans. NeuroImage 34 (1), 426–434. http://dx.doi.org/10.1016/j.neuroimage.2006.07.018.
Heidemann, R.M., Porter, D.A., Anwander, A., Feiweier, T., Heberlein, K., Knösche, T.R., Turner, R., 2010. Diffusion imaging in humans at 7 T using readout-segmented EPI and GRAPPA. Magn. Reson. Med. 64 (1), 9–14. http://dx.doi.org/10.1002/mrm.22480.
Heim, S., Eickhoff, S.B., Amunts, K., 2008. Specialisation in Broca's region for semantic, phonological, and syntactic fluency? NeuroImage 40 (3), 1362–1368. http://dx.doi.org/10.1016/j.neuroimage.2008.01.009.
Heim, S., van Ermingen, M., Huber, W., Amunts, K., 2010. Left cytoarchitectonic BA 44 processes syntactic gender violations in determiner phrases. Hum. Brain Mapp. 31 (10), 1532–1541. http://dx.doi.org/10.1002/hbm.20957.
Hickok, G., Okada, K., Serences, J.T., 2008. Area Spt in the human planum temporale supports sensory-motor integration for speech processing. J. Neurophysiol. 101 (5), 2725–2732. http://dx.doi.org/10.1152/jn.91099.2008.
Hickok, G., Buchsbaum, B., Humphries, C., Muftuler, T., 2003. Auditory–motor interaction revealed by fMRI: speech, music, and working memory in area Spt. J. Cogn. Neurosci. 15 (5), 673–682. http://dx.doi.org/10.1162/jocn.2003.15.5.673.
Howell, P., Au-Yeung, J., 2002. The EXPLAN theory of fluency control and the diagnosis of stuttering. In: Fava, E. (Ed.), Pathology and Therapy of Speech Disorders. John Benjamins, Amsterdam, pp. 75–94.
Huber, L., Goense, J., Kennerley, A.J., Trampel, R., Guidi, M., Reimer, E., ... Möller, H.E., 2015. Cortical lamina-dependent blood volume changes in human brain at 7 T. NeuroImage 107, 23–33. http://dx.doi.org/10.1016/j.neuroimage.2014.11.046.
Ingham, R.J., Fox, P.T., Ingham, J.C., Xiong, J., Zamarripa, F., Hardies, L.J., Lancaster, J.L., 2004. Brain correlates of stuttering and syllable production: gender comparison and replication. Journal of Speech, Language, and Hearing Research 47 (2), 321–341. http://dx.doi.org/10.1044/1092-4388(2004/026).
Ingham, R.J., Grafton, S.T., Bothe, A.K., Ingham, J.C., 2012. Brain activity in adults who stutter: similarities across speaking tasks and correlations with stuttering frequency and speaking rate. Brain Lang. 122 (1), 11–24. http://dx.doi.org/10.1016/j.bandl.2012.04.002.
Jeffries, K.J., Fritz, J.B., Braun, A.R., 2003. Words in melody: an H(2)15O PET study of brain activation during singing and speaking. Neuroreport 14 (5), 749–754. http://dx.doi.org/10.1097/01.wnr.0000066198.94941.a4.
Jenkinson, M., Smith, S., 2001. A global optimisation method for robust affine registration of brain images. Med. Image Anal. 5 (2), 143–156. http://dx.doi.org/10.1016/S1361-8415(01)00036-6.
Jenkinson, M., Bannister, P., Brady, M., Smith, S., 2002. Improved optimization for the robust and accurate linear registration and motion correction of brain images. NeuroImage 17 (2), 825–841. http://dx.doi.org/10.1006/nimg.2002.1132.
Jeon, H.-A., Friederici, A.D., 2013. Two principles of organization in the prefrontal cortex are cognitive hierarchy and degree of automaticity. Nat. Commun. 4, 2041. http://dx.doi.org/10.1038/ncomms3041.
Jeon, H.-A., Friederici, A.D., 2015. Degree of automaticity and the prefrontal cortex. Trends Cogn. Sci. 19 (5), 244–250. http://dx.doi.org/10.1016/j.tics.2015.03.003.
Kell, C.A., Neumann, K., von Kriegstein, K., Posenenske, C., von Gudenberg, A.W., Euler, H., Giraud, A.-L., 2009. How the brain repairs stuttering. Brain 132 (10), 2747–2760. http://dx.doi.org/10.1093/brain/awp185.
Kent, R.D., 2000. Research on speech motor control and its disorders: a review and prospective. J. Commun. Disord. 33 (5), 391–428.
Kikuchi, Y., Ogata, K., Umesaki, T., Yoshiura, T., Kenjo, M., Hirano, Y., ... Tobimatsu, S., 2011. Spatiotemporal signatures of an abnormal auditory system in stuttering. NeuroImage 55 (3), 891–899. http://dx.doi.org/10.1016/j.neuroimage.2010.12.083.
Kleber, B., Veit, R., Birbaumer, N., Gruzelier, J., Lotze, M., 2010. The brain of opera singers: experience-dependent changes in functional activation. Cereb. Cortex 20 (5), 1144–1152. http://dx.doi.org/10.1093/cercor/bhp177.
Koechlin, E., Summerfield, C., 2007. An information theoretical approach to prefrontal executive function. Trends Cogn. Sci. 11 (6), 229–235. http://dx.doi.org/10.1016/j.tics.2007.04.005.
Koechlin, E., Danek, A., Burnod, Y., Grafman, J., 2002. Medial prefrontal and subcortical mechanisms underlying the acquisition of motor and cognitive action sequences in humans. Neuron 35 (2), 371–381. http://dx.doi.org/10.1016/S0896-6273(02)00742-0.
Koelsch, S., Gunter, T.C., von Cramon, D.Y., Zysset, S., Lohmann, G., Friederici, A.D., 2002. Bach speaks: a cortical "language-network" serves the processing of music. NeuroImage 17 (2), 956–966. http://dx.doi.org/10.1006/nimg.2002.1154.
Koelsch, S., Schulze, K., Sammler, D., Fritz, T., Müller, K., Gruber, O., 2009. Functional architecture of verbal and tonal working memory: an FMRI study. Hum. Brain Mapp. 30 (3), 859–873. http://dx.doi.org/10.1002/hbm.20550.

Konoike, N., Kotozaki, Y., Miyachi, S., Miyauchi, C.M., Yomogida, Y., Akimoto, Y., ... Nakamura, K., 2012. Rhythm information represented in the fronto-parieto-cerebellar motor system. NeuroImage 63 (1), 328–338. http://dx.doi.org/10.1016/j.neuroimage.2012.07.002.

Kronfeld-Duenias, V., Amir, O., Ezrati-Vinacour, R., Civier, O., Ben-Shachar, M., 2014. The frontal aslant tract underlies speech fluency in persistent developmental stuttering. Brain Struct. Func. http://dx.doi.org/10.1007/s00429-014-0912-8.

Laird, A.R., Eickhoff, S.B., Kurth, F., Fox, P.M., Uecker, A.M., Turner, J.A., ... Fox, P.T., 2009. ALE meta-analysis workflows via the Brainmap database: progress towards a probabilistic functional brain atlas. Front. Neuroinformatics 3. http://dx.doi.org/10.3389/neuro.11.023.2009.

Lancaster, J.L., Woldorff, M.G., Parsons, L.M., Liotti, M., Freitas, C.S., Rainey, L., ... Fox, P.T., 2000. Automated Talairach atlas labels for functional brain mapping. Hum. Brain Mapp. 10 (3), 120–131. http://dx.doi.org/10.1002/1097-0193(200007)10:3<120::AID-HBM30>3.0.CO;2-8.

Levy, B.J., Wagner, A.D., 2011. Cognitive control and right ventrolateral prefrontal cortex: reflexive reorienting, motor inhibition, and action updating. Ann. N. Y. Acad. Sci. 1224 (1), 40–62. http://dx.doi.org/10.1111/j.1749-6632.2011.05958.x.

Lu, C., Chen, C., Peng, D., You, W., Zhang, X., Ding, G., ... Howell, P., 2012. Neural anomaly and reorganization in speakers who stutter: a short-term intervention study. Neurology 79 (7), 625–632. http://dx.doi.org/10.1212/WNL.0b013e31826356d2.

Ludlow, C.L., 2000. Stuttering: dysfunction in a complex and dynamic system. Brain 123 (10), 1983–1984. http://dx.doi.org/10.1093/brain/123.10.1983.

Maguire, G.A., Yu, B.P., Franklin, D.L., Riley, G.D., 2004. Alleviating stuttering with pharmacological interventions. Expert. Opin. Pharmacother. 5 (7), 1565–1571. http://dx.doi.org/10.1517/14656566.5.7.1565.

Maguire, G., Franklin, D., Vatakis, N.G., Morgenshtern, E., Denko, T., Yaruss, J.S., ... Riley, G., 2010. Exploratory randomized clinical study of pagoclone in persistent developmental stuttering. J. Clin. Psychopharmacol. 30 (1), 48–56. http://dx.doi.org/10.1097/JCP.0b013e3181caebbe.

Majid, D.S.A., Cai, W., Corey-Bloom, J., Aron, A.R., 2013. Proactive selective response suppression is implemented via the basal ganglia. J. Neurosci. 33 (33), 13259–13269. http://dx.doi.org/10.1523/JNEUROSCI.5651-12.2013.

Max, L., Guenther, F.H., Gracco, V.L., Ghosh, S.S., Wallace, M.E., 2004. Unstable or insufficiently activated internal models and feedback-biased motor control as sources of dysfluency: a theoretical model of stuttering. Contemporary Issues in Communication Science and Disorders, pp. 105–122.

Murphy, D.G.M., DeCarli, C., McIntosh, A.R., Daly, E., Mentis, M.J., Pietrini, P., ... Rapoport, S.I., 1996. Sex differences in human brain morphometry and metabolism: an in vivo quantitative magnetic resonance imaging and positron emission tomography study on the effect of aging. Arch. Gen. Psychiatry 53 (7), 585–594. http://dx.doi.org/10.1001/archpsyc.1996.01830070031007.

Neef, N.E., Jung, K., Rothkegel, H., Pollok, B., von Gudenberg, A.W., Paulus, W., Sommer, M., 2011a. Right-shift for non-speech motor processing in adults who stutter. Cortex 47 (8), 945–954. http://dx.doi.org/10.1016/j.cortex.2010.06.007.

Neef, N.E., 2013. Reduced dynamic range to tune the sensory-motor coupling on the left, at least in males who stutter. Presented at the ASHA Convention 2013 - Updated Perspectives on the Neural Bases of Stuttering: Sensory & Motor Mechanisms Underlying Dysfluent Speech, November 14–16, 2013, Chicago.

Neef, N., Anwander, A., Friederici, A.D., 2015a. The neurobiological grounding of persistent stuttering: from structure to function. Current Neurology and Neuroscience Reports 15 (9), 1–11. http://dx.doi.org/10.1007/s11910-015-0579-4.

Neef, N.E., Paulus, W., Neef, A., von Gudenberg, A.W., Sommer, M., 2011b. Reduced intracortical inhibition and facilitation in the primary motor tongue representation of adults who stutter. Clin. Neurophysiol. 122 (9), 1802–1811. http://dx.doi.org/10.1016/j.clinph.2011.02.003.

Neef, N.E., Hoang, T.N.L., Neef, A., Paulus, W., Sommer, M., 2015b. Speech dynamics are coded in the left motor cortex in fluent speakers but not in adults who stutter. Brain 138 (3), 712–725. http://dx.doi.org/10.1093/brain/awu390.

Neumann, K., Preibisch, C., Euler, H.A., von Gudenberg, A.W., Lanfermann, H., Gall, V., Giraud, A.-L., 2005. Cortical plasticity associated with stuttering therapy. J. Fluen. Disord. 30 (1), 23–39. http://dx.doi.org/10.1016/j.jfludis.2004.12.002.

Nishitani, N., Hari, R., 2000. Temporal dynamics of cortical representation for action. Proc. Natl. Acad. Sci. 97 (2), 913–918. http://dx.doi.org/10.1073/pnas.97.2.913.

O'Reilly, J.X., Woolrich, M.W., Behrens, T.E.J., Smith, S.M., Johansen-Berg, H., 2012. Tools of the trade: psychophysiological interactions and functional connectivity. Soc. Cogn. Affect. Neurosci. 7 (5), 604–609. http://dx.doi.org/10.1093/scan/nss055.

Oldfield, R.C., 1971. The assessment and analysis of handedness: the Edinburgh inventory. Neuropsychologia 9 (1), 97–113. http://dx.doi.org/10.1016/0028-3932(71)90067-4.

Özdemir, E., Norton, A., Schlaug, G., 2006. Shared and distinct neural correlates of singing and speaking. NeuroImage 33 (2), 628–635. http://dx.doi.org/10.1016/j.neuroimage.2006.07.013.

Palmer, E.D., Rosen, H.J., Ojemann, J.G., Buckner, R.L., Kelley, W.M., Petersen, S.E., 2001. An event-related fMRI study of overt and covert word stem completion. NeuroImage 14 (1), 182–193. http://dx.doi.org/10.1006/nimg.2001.0779.

Penhune, V.B., Doyon, J., 2002. Dynamic cortical and subcortical networks in learning and delayed recall of timed motor sequences. J. Neurosci. 22 (4), 1397–1406.

Platel, H., Price, C., Baron, J.C., Wise, R., Lambert, J., Frackowiak, R.S., ... Eustache, F., 1997. The structural components of music perception. A functional anatomical study. Brain 120 (2), 229–243. http://dx.doi.org/10.1093/brain/120.2.229.

Preibisch, C., Neumann, K., Raab, P., Euler, H.A., von Gudenberg, A.W., Lanfermann, H., Giraud, A.-L., 2003. Evidence for compensation for stuttering by the right frontal operculum. NeuroImage 20 (2), 1356–1364. http://dx.doi.org/10.1016/S1053-8119(03)00376-8.

Price, C.J., 2010. The anatomy of language: a review of 100 fMRI studies published in 2009. Ann. N. Y. Acad. Sci. 1191 (1), 62–88. http://dx.doi.org/10.1111/j.1749-6632.2010.05444.x.

Ranganath, C., Johnson, M.K., D'Esposito, M., 2003. Prefrontal activity associated with working memory and episodic long-term memory. Neuropsychologia 41 (3), 378–389. http://dx.doi.org/10.1016/S0028-3932(02)00169-0.

Riecker, A., Ackermann, H., Wildgruber, D., Dogil, G., Grodd, W., 2000. Opposite hemispheric lateralization effects during speaking and singing at motor cortex, insula and cerebellum. [miscellaneous article]. Neuroreport 11 (9), 1997–2000.

Riecker, A., Kassubek, J., Gröschel, K., Grodd, W., Ackermann, H., 2006. The cerebral control of speech tempo: opposite relationship between speaking rate and BOLD signal changes at striatal and cerebellar structures. NeuroImage 29 (1), 46–53. http://dx.doi.org/10.1016/j.neuroimage.2005.03.046.

Riley, G.D., 2008. Stuttering Severity Instrument, Fourth Edition (SSI-4). fourth edition. Pearson Education.

Sahin, N.T., Pinker, S., Cash, S.S., Schomer, D., Halgren, E., 2009. Sequential processing of lexical, grammatical, and phonological information within Broca's area. Science 326 (5951), 445–449. http://dx.doi.org/10.1126/science.1174481.

Sakai, K., Passingham, R.E., 2006. Prefrontal set activity predicts rule-specific neural processing during subsequent cognitive performance. J. Neurosci. 26 (4), 1211–1218. http://dx.doi.org/10.1523/JNEUROSCI.3887-05.2006.

Salmelin, R., Schnitzler, A., Schmitz, F., Freund, H.-J., 2000. Single word reading in developmental stutterers and fluent speakers. Brain 123 (6), 1184–1202. http://dx.doi.org/10.1093/brain/123.6.1184.

Smith, S.M., 2002. Fast robust automated brain extraction. Hum. Brain Mapp. 17 (3), 143–155. http://dx.doi.org/10.1002/hbm.10062.

Smith, A., Kelly, E., 1997. Stuttering: a dynamic multifactorial model. In: Curlee, R., Siegel, G. (Eds.), Nature and Treatment of Stuttering: New Directions, 2nd ed Allyn & Bacon, Needham Heigts, MA, pp. 204–217.

Smith, A., Zelaznik, H.N., 2004. Development of functional synergies for speech motor coordination in childhood and adolescence. Dev. Psychobiol. 45 (1), 22–33. http://dx.doi.org/10.1002/dev.20009.

Sommer, M., Classen, J., Cohen, L.G., Hallett, M., 2001. Time course of determination of movement direction in the reaction time task in humans. J. Neurophysiol. 86 (3), 1195–1201.

Stager, S.V., Jeffries, K.J., Braun, A.R., 2003. Common features of fluency-evoking conditions studied in stuttering subjects and controls: an H215O PET study. J. Fluen. Disord. 28 (4), 319–336. http://dx.doi.org/10.1016/j.jfludis.2003.08.004.

Stinear, C.M., Coxon, J.P., Byblow, W.D., 2009. Primary motor cortex and movement prevention: where stop meets go. Neurosci. Biobehav. Rev. 33 (5), 662–673. http://dx.doi.org/10.1016/j.neubiorev.2008.08.013.

Swann, N., Tandon, N., Canolty, R., Ellmore, T.M., McEvoy, L.K., Dreyer, S., ... Aron, A.R., 2009. Intracranial EEG reveals a time- and frequency-specific role for the right inferior frontal gyrus and primary motor cortex in stopping initiated responses. J. Neurosci. 29 (40), 12675–12685. http://dx.doi.org/10.1523/JNEUROSCI.3359-09.2009.

Thoenissen, D., Zilles, K., Toni, I., 2002. Differential involvement of parietal and precentral regions in movement preparation and motor intention. J. Neurosci. 22 (20), 9024–9034.

Tian, X., Zarate, J.M., Poeppel, D., 2016. Mental imagery of speech implicates two mechanisms of perceptual reactivation. Cortex 77, 1–12. http://dx.doi.org/10.1016/j.cortex.2016.01.002.

Toft, M., Dietrichs, E., 2011. Aggravated stuttering following subthalamic deep brain stimulation in Parkinson's disease - two cases. BMC Neurol. 11, 44. http://dx.doi.org/10.1186/1471-2377-11-44.

Tourville, J.A., Reilly, K.J., Guenther, F.H., 2008. Neural mechanisms underlying auditory feedback control of speech. NeuroImage 39 (3), 1429–1443. http://dx.doi.org/10.1016/j.neuroimage.2007.09.054.

Toyomura, A., Fujii, T., Kuriki, S., 2011. Effect of external auditory pacing on the neural activity of stuttering speakers. NeuroImage 57 (4), 1507–1516. http://dx.doi.org/10.1016/j.neuroimage.2011.05.039.

Toyomura, A., Fujii, T., Kuriki, S., 2015. Effect of an 8-week practice of externally triggered speech on basal ganglia activity of stuttering and fluent speakers. NeuroImage 109, 458–468. http://dx.doi.org/10.1016/j.neuroimage.2015.01.024.

Tsuboi, T., Watanabe, H., Tanaka, Y., Ohdake, R., Yoneyama, N., Hara, K., ... Sobue, G., 2015. Distinct phenotypes of speech and voice disorders in Parkinson's disease after subthalamic nucleus deep brain stimulation. Journal of Neurology Neurosurgery and Psychiatry 86 (8), 856–864. http://dx.doi.org/10.1136/jnnp-2014-308043.

Tykalová, T., Rusz, J., Čmejla, R., Klempíř, J., Růžičková, H., Roth, J., Růžička, E., 2015. Effect of dopaminergic medication on speech dysfluency in Parkinson's disease: a longitudinal study. J. Neural Transm. 122 (8), 1135–1142. http://dx.doi.org/10.1007/s00702-015-1363-y.

Uddén, J., Bahlmann, J., 2012. A rostro-caudal gradient of structured sequence processing in the left inferior frontal gyrus. Philosophical Transactions of the Royal Society B: Biological Sciences 367 (1598), 2023–2032. http://dx.doi.org/10.1098/rstb.2012.0009.

Uddin, L.Q., Supekar, K., Amin, H., Rykhlevskaia, E., Nguyen, D.A., Greicius, M.D., Menon, V., 2010. Dissociable connectivity within human angular gyrus and intraparietal sulcus: evidence from functional and structural connectivity. Cereb. Cortex 20 (11), 2636–2646. http://dx.doi.org/10.1093/cercor/bhq011.

van Lieshout, P., Hulstijn, W., Peters, H., Van Lieshout, P., Hulstijn, W., 2004. Searching for the weak link in the speech production chain of people who stutter: a motor skill approach. In: Maassen, B., Kent, R., Peters, H.F.M., Maassen, B., Kent, R., Peters, H.F.M., van Lieshout, P., Hulstijn, W. (Eds.), Speech Motor Control in Normal and Disordered Speech. Oxford University Press, New York.

Vanhoutte, S., Cosyns, M., van Mierlo, P., Batens, K., Corthals, P., De Letter, M., ... Santens, P., 2016. When will a stutterwing moment occur? The determining role of speech motor preparation. Neuropsychologia http://dx.doi.org/10.1016/j.neuropsychologia.2016.04.018 (n.d.).

Walker, H.C., Phillips, D.E., Boswell, D.B., Guthrie, B.L., Guthrie, S.L., Nicholas, A.P., ... Watts, R.L., 2009. Relief of acquired stuttering associated with Parkinson's disease by unilateral left subthalamic brain stimulation. J. Speech Lang. Hear. Res. 52 (6), 1652–1657.

Walsh, B., Mettel, K.M., Smith, A., 2015. Speech motor planning and execution deficits in early childhood stuttering. J. Neurodev. Disord. 7, 27. http://dx.doi.org/10.1186/s11689-015-9123-8.

Watkins, K.E., Smith, S.M., Davis, S., Howell, P., 2008. Structural and functional abnormalities of the motor system in developmental stuttering. Brain 131 (1), 50–59. http://dx.doi.org/10.1093/brain/awm241.

Wiecki, T.V., Frank, M.J., 2013. A computational model of inhibitory control in frontal cortex and basal ganglia. Psychol. Rev. 120 (2), 329–355. http://dx.doi.org/10.1037/a0031542.

Worsley, K.J., 2001. Statistical analysis of activation images. In: Jezzard, P., Matthews, P.M., Smith, S.M. (Eds.), Functional MRI: An Introduction to Methods. OUP.

Worsley, K.J., Evans, A.C., Marrett, S., Neelin, P., 1996. A three-dimensional statistical analysis for CBF activation studies in human brain. J. Cereb. Blood Flow Metab. 12 (6), 900–918. http://dx.doi.org/10.1038/jcbfm.1992.127.

Wu, J.C., Maguire, G., Riley, G., Fallon, J., LaCasse, L., Chin, S., ... Lottenberg, S., 1995. A positron emission tomography [18F]deoxyglucose study of developmental stuttering. Neuroreport 6 (3), 501–505. http://dx.doi.org/10.1097/00001756-199502000-00024.

Wu, J.C., Maguire, G., Riley, G., Lee, A., Keator, D., Tang, C., ... Najafi, A., 1997. Increased dopamine activity associated with stuttering. Neuroreport 8 (3), 767–770. http://dx.doi.org/10.1097/00001756-199702100-00037.

Wymbs, N.F., Ingham, R.J., Ingham, J.C., Paolini, K.E., Grafton, S.T., 2013. Individual differences in neural regions functionally related to real and imagined stuttering. Brain Lang. 124 (2), 153–164. http://dx.doi.org/10.1016/j.bandl.2012.11.013.

Xue, G., Aron, A.R., Poldrack, R.A., 2008. Common neural substrates for inhibition of spoken and manual responses. Cereb. Cortex 18 (8), 1923–1932. http://dx.doi.org/10.1093/cercor/bhm220.

Yang, Y., Jia, F., Siok, W.T., Tan, L.H., 2016. Altered functional connectivity in persistent developmental stuttering. Sci. Rep. 6, 19128. http://dx.doi.org/10.1038/srep19128.

Yeo, B.T.T., Krienen, F.M., Sepulcre, J., Sabuncu, M.R., Lashkari, D., Hollinshead, M., ... Buckner, R.L., 2011. The organization of the human cerebral cortex estimated by intrinsic functional connectivity. J. Neurophysiol. 106 (3), 1125–1165. http://dx.doi.org/10.1152/jn.00338.2011.